İSTANBUL TECHNICAL UNIVERSITY ★ INSTITUTE OF SCIENCE AND TECHNOLOGY

DESIGN and IMPLEMENTATION of PERMANENT MAGNET BRUSHLESS DC MOTOR

M.Sc. Thesis by
Kadir ERDEM

Department : Mechatronic Engineering

Programme : Mechatronic Engineering

Thesis Supervisor: Assist. Prof. Dr. Özgür ÜSTÜN

SEPTEMBER 2011

İSTANBUL TECHNICAL UNIVERSITY ★ INSTITUTE OF SCIENCE AND TECHNOLOGY

DESIGN and IMPLEMENTATION of PERMANENT MAGNET BRUSHLESS DC MOTOR

M.Sc. Thesis by
Kadir ERDEM
(518081016)

Date of submission : 12 September 2011
Date of defence examination: 22 September 2011

Supervisor (Chairman) : Assist. Prof. Dr. Özgür ÜSTÜN (İTÜ)
Members of the Examining Committee : Prof. Dr. Metin GÖKAŞAN (İTÜ)
Assist Prof. Dr. Levent OVACIK (İTÜ)

SEPTEMBER 2011

İSTANBUL TEKNİK ÜNİVERSİTESİ ★ FEN BİLİMLERİ ENSTİTÜSÜ

SÜREKLİ MIKNATISLI DOĞRU AKIM MOTORU TASARIMI ve UYGULAMASI

YÜKSEK LİSANS TEZİ
Kadir ERDEM
(518081016)

Tezin Enstitüye Verildiği Tarih : 12 Eylül 2011
Tezin Savunulduğu Tarih : 22 Eylül 2011

Tez Danışmanı : Assist. Prof. Özgür ÜSTÜN (İTÜ)
Diğer Jüri Üyeleri : Prof. Dr. Metin GÖKAŞAN (İTÜ)
Assist Prof. Dr. Levent OVACIK (İTÜ)

EYLÜL 2011

FOREWORD

First of all, I would like to thank to my thesis advisor *Assist. Prof. Dr. Özgür ÜSTÜN* for his assistance, encouragements and advices throughout the project.

I would like to thank to TUBITAK-BIDEB for their support during the period of my master science education.

I also would like to express my deep appreciation to all my lecturers who have made invaluable contribution to my education.

I would like to thank to *Aksa Motor Fan* Company that helped me in the manufacturing of the mechanical parts used in the project.

Lastly, I would like to express my heartfelt thanks to my family and all of my friends.

September 2011

Kadir ERDEM

(Electrical & Electronic Engineer)
(Mechanical Engineer)

TABLE OF CONTENTS

Page

ABBREVIATIONS

BLDC **:** Brushless Direct Current
PMBLDC **:** Permanent Magnet Brushless Direct Current
NdFeB **:** Neodymium Iron Boron
SmCo **:** Samarium Cobalt
FEM **:** Finite element method
EMF **:** Electro-motive force
MGOe **:** Mega Gauss-Oersted

LIST OF TABLES

Page

LIST OF FIGURES

Page

LIST OF SYMBOLS

B	**:** Magnetic flux density
H_c	**:** Magnetic field intensity
μ	**:** Permeability of a material
Ø	**:** Total magnetic flux
ψ	**:** Magneto motive force
F	**:** Force generated on electric current
P_m	**:** Permeance of a magnet
T_{curie}	**:** Curie temperature of permanent magnet
BH_{max}	**:** Energy product of permanent magnet
Br	**:** Residual magnetic flux density
T_{FAN}	**:** Torque of fan
I_L	**:** Current with load
I_O	**:** Current without load

DESIGN and IMPLEMENTATION of PERMANENT MAGNET BRUSHLESS DC MOTOR

SUMMARY

In this project, design and implementation of single-phase permanent magnet brushless direct current (PMBLDC) motor for low power fan application will be considered. The design is divided into two main steps: First step includes the mechanical design and second step comprises the magnetic design. All stages are divided into sub-stages including details of each design steps. Impeller and housing of the fan are designed in the first phase. The dimensions are determined as a result of the FEM simulations. In the second phase, the magnetic analysis of the motor is achieved with different motor structure in order to get the optimum motor characteristic for the load obtained in the mechanical phase.

Firstly, mechanical parts of the fan are designed by using 3-D design program. Then both the environment in which the PMBLDC fan motor will work and the mechanical parts are designed and simulated. Three different designs are modeled and simulated. Their results are compared and the optimum design is achieved. The optimum design obtained by using FEM techniques is also experimentally realized. The torque-speed characteristic of the fan is derived by experimentally and the simulation and experimental results are compared with each other to see the effectiveness of the simulation. As a result of this work, design parameters are determined for the single-phase PMBLDC motor.

Magnetic model of the PMBLDC motor is determined according to the FEM analyses. Three different design approaches are applied and effective results are obtained. The torque output, current waveforms, flux linkages and back emfs of the motors are examined in details. The magnetic field distribution in the stator, rotor and magnet are observed and some improvements are achieved by comparing the result of these designs. The effectiveness of the asymmetric air gap model is implied while the motor has same number of stator and magnet poles. The influence of the switching angle on the motor performance is analyzed and the optimum switching angle is determined.

Finally, uni-directional PMBLDC motor with asymmetric air gap was chosen for the mechanical load obtained in the first phase of the project. The design results obtained in the magnetic analysis phase are compared with the results obtained in the mechanical analysis phase and satisfactory results are achieved. It is observed that the characteristics of the designed single-phase PMBLDC motor are fulfilling the needs of the mechanical load.

SÜREKLİ MIKNATISLI FIRÇASIZ DOĞRU AKIM MOTOR TASARIMI VE UYGULAMASI

ÖZET

Bu projede düşük güç uygulamalarında kullanılmak üzere tek fazlı sabit mıknatıslı fırçasız doğru akım motoru (SMFDAM) tasarımı ve uygulaması ele alınmıştır. Proje iki önemli adımda hazırlanmıştır. Birinci fazda motorun mekanik tasarımı yapılmış ikinci fazda ise bu tasarıma uygun tek fazlı SMFDAM motorunun manyetik tasarımı ele alınmıştır. Bu adımlar kendi içlerinde tasarım ayrıntılarına göre birçok adıma ayrılmaktadırlar. Projenin birinci kısmında, fan ve fana ait gövde tasarımı yapılmıştır ve sonlu elemenlar yöntemleri (SEY) kullanılarak en optimum ölçüler elde edilmiştir. İkinci fazda ise en iyi motor karakteristiğini elde edebilmek için farklı motor yapıları tasarlanmış ve bu tasarımlar SEY'iyle manyetik açıdan irdelenmiştir.

Birinci fazda, mekanik parçalar 3D tasarım programı yardımıyla tasarlanmıştır. Elde edilen fan ve gövde yine 3D ortamında gerçeğe çok yakın olarak oluşturulan ortama konularak mekanik açıdan simule edilmiştir. Elde edilen sonuçlara göre motor için kullanılacak fan ve gövde düzenlenerek en optimum sonuçlar elde edilmeye çalışılmıştır. Similasyon sonucunda elde edilen optimum tasarım (fan ve gövde) gerçeklenerek deneysel ölçülmlerde kullanılmıştır. Fana ait tork ve hız eğrisi deneysel olarak çıkarılmış ve simulasyondan elde edilen tork-hız eğrisiyle kıyaslanarak simulasyon sonuçlarının gerçek koşullara yakınlığı gözlenmiştir. Bu çalışmaların sonucunda, tek fazlı SMFDAM motor için tasarım parametreleri çıkarlarak ikinci faz için gerekli olan veriler hazır hale getirilmiştir.

Projenin ikinci fazında, mekanik tasarımların sonucunda elde edilen verilere uygun motor tasarımına başlanmıştır. SEY sonuçlarına göre SMFDAM motorunun manyetik modelleri belirlenmeye çalışılmıştır. Değişik motor yapıları kullanılmış ve etkili sonuçlar elde edilmiştir. Sonuçlar tork, akım dalga şekli, akı halkası, ters elektromotor kuvveti (emf) parametreleri ışığında incelenmiştir. Ayrıca stator, rotor ve mıknatıs üzerindeki manyetik alan dağılımları detaylı olarak incelenmiştir. Elde edilen sonuçlar kıyaslanarak, yapılan iyileştirmeler ile tasarımda önemli başarılar elde edilmiştir.Özellikle asimetrik hava boşluğu üzerinde yoğunlaşılmış ve aynı kutup sayısına sahip mıknatıs ve stator için asimetrik hava boşluğu tasarımının önemi vurgulanmıştır. Ayrıca, akımın, rotor hangi açıdayken yön değiştimesi gerektiği irdelenmiş ve motor veriminin en yüksek olduğu akım tetikleme açısı belirlenmiştir.

Son olarak, projenin birinci fazında elde edilen fan yükü için asimetrik hava boşluğun sahip tek yönlü SMFDAM modeli seçilmiştir. Manyetik analiz fazında elde edilen sonuçlar ile mekanik tasarım sonuçları bir araya getirilerek karşılaştırma yapılmıştır ve tatmin edici sonuçlar elde edilmiştir.

1. INTRODUCTION

Motors are widely used in every area in human being's lives. It is easy to see different applications of motors in everywhere from aspirators in a bathroom to milling machines in industrial factories. While the motors have been becoming indispensable parts of both domestic and industrial applications, it becomes crucial to consider motors in terms of cost, energy efficiency and manufacturing methods. There are various types of motors available in the markets, which are classified mainly under two groups: AC and DC Motors. After Tesla invented the alternating current motors, they become very common in the market. Even though AC motors have some advantages such as simple design and easy maintenance, attentions are attracted on DC motors because of their simple drive circuit and easiness of torque and speed control. DC motors become commonly used in several applications at the same time they creates some problems such as dust contamination and brush wear which lead to make investigations on Brushless Direct Current Motors (BLDC). BLDC motors have experienced an outstanding development after revolution is achieved in power electronics, microcontrollers, and permanent magnets.

BLDC motors come forward with several practical advantages. The disadvantages found with mechanical commutators, such as wear of the commutating device, brush wear, carbon dust contamination due to abrasion, starting difficulties because of commutator corrosion or spark formation are avoided. Besides, BLDC motors with their simplified structure have linear torque/speed characteristics and are easy to control. They offer high efficiency, silent operation, and lower excitation losses with their maintenance–free operation.

BLDC motors are also knows as Electronically Commutated (EC) motors. This is because while the rotational motion is accomplished by using mechanical commutators and brushes in Brushed DC motors, in BLDC motors the commutation is achieved by electronic switches. Magnetic field formed due current excitation on

stator and permanent magnetic field due to magnets on the rotor come together to generate continuous rotational motion.

BLDC motors are also extensively used in Heating, Cooling and Ventilating applications (HVAC). Since BLCD motors have advantages such as easy control, compact size, and maintenance-free operation, they are commonly used in especially low power ventilating applications such as aspirators in our bathrooms, tangential cross flow blowers in vertical refrigerators and cooling fans used in computer cases and server chassis. With advantages mentioned previously, the most important reason why BLDC motors are used in fan application is that fan applications require high efficiency torque/speed characteristic. Generally, one is looking for fan motors with 'rigid' motor characteristics, which just means that the motor speed hardly alters over the total fan curve. In other words, the speed of the motor should only demonstrate minimal fluctuations, even though the torque requirement of the fan is changing dependent on the operating conditions. In the following part, roles of BLDC motors in ventilating applications will be discussed with examples.

1.1 Brushless Direct Current (BLDC) Motor Technologies for Ventilation Applications

Modern fans are now generally all equipped with small, BLDC motors. This kind of simple motor is considerably more cost-effective than the AC asynchronous types that were often used before. Fan speeds from 1,000 up to 6,000 rpm are now a possibility – in special cases, this can be extended up to 60,000 rpm and even higher. Moreover, the efficiency factor of DC drives is significantly higher than with AC motors. Unfortunately, these small motors do have a weakness, which results in the typical saddle effect as shown in the static pressure / flow rate diagram in figure-1.1. In free air operation, an axial fan has its lowest torque requirement and the motor its highest speed. As the counter pressure rises, so the energy requirement of the fan impeller increases and the motor can no longer maintain the speed. To a certain extent electronic correction of the motor can be of help here [1].

For years brushless DC tube axial (box) fans have been growing in use, importance and market share for cooling electronics in cabinets and enclosures for computers, telecommunications and medical equipment. As more electronics, at higher package

densities, are incorporated into appliances the impact, value and benefits of brushless DC are creating more and more interest for brushless DC in traditional AC applications. It has long been common knowledge that DC motor technology offers specific user advantages versus AC:

- Total and simplified speed control
- Linear speed/torque relationship
- Motor efficiencies up to about 4 times higher versus comparable AC units

Motors used in air moving devices and the resultant performance of fans and blowers are perfect illustrations for the true benefits of brushless DC versus AC performance. The benefits of designing and specifying brushless DC blowers as an alternative to standard fans also become self-evident (Table 1.1) [1].

Table 1.1: Comparison table of the BLDC motor fan and AC motor fan with examples

Product No	Product Name	Flow Rate (CFM)	Sound Level (dBA)	Power (Watts)	Maximum Temperature (^{0}C)
1	5.25” standard brushless DC motorized impeller	174	62	21	50
2	5.25” standard AC motorized impeller	170	60	45	55
3	5.31” DC tubeaxial (box) fan	147	48	9.5	72
4	5.31” AC tubeaxial fan	159	50	26	80
5	Fan Tray with three brushless DC fans	300	50	15	75
6	Fan tray with three AC fans	318	56	54	60

All fans and blowers are rated and listed for specification as operating at zero static pressure (back pressure) and pressure is usually calculated using inches of water as the measurement. In reality, every application whether in an enclosure, in duct work for ventilating, or on a ceiling or wall for an exhaust application deals with static pressure. Pressure is resistance the air-moving device encounters in pulling air into or pushing the air out and through the exhaust side of the fan or blower. The air performance graph plotting the performance of each product below shows the CFM versus Static Pressure for each product (figure-1.1).

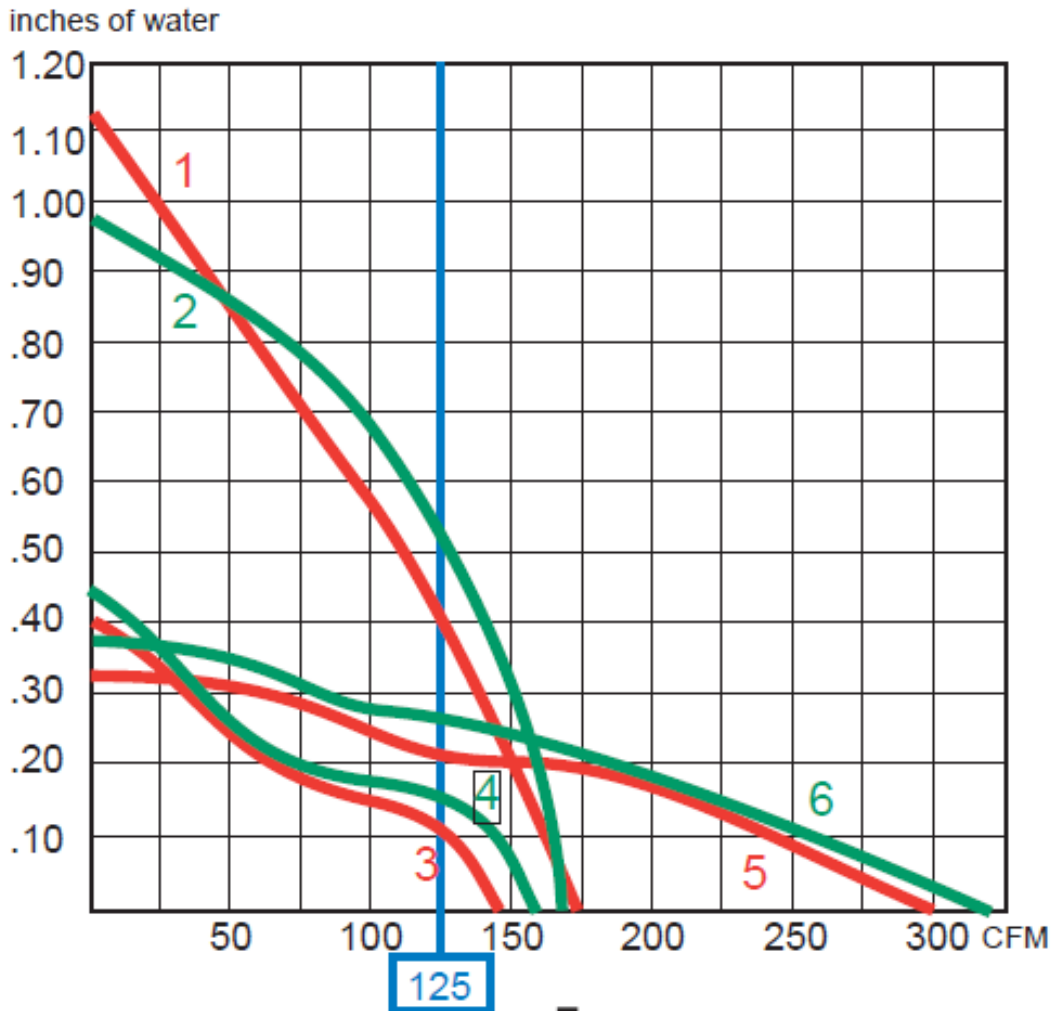

Figure 1.1 : Pressure & airflow rate comparison of the BLDC motor fan and AC motor fan

If we select a CFM operating point of 125 CFM, look at the performance capabilities of each product relative to static pressure. As long as static pressures are very low, the fans stay in the ball game, but as pressures rise blowers become the best choice, because even adding more fans in a fan tray will not satisfy the air power needed to move air effectively against a higher static pressure. Just to summarize the graph in table form, for the 125 CFM operating point that is desired, it is easy to evaluate the advantage of motorized impellers. At an operating point of 125 CFM the static pressures (in H_2O) for each product are as follows (table-1.2):

Table 1.2: Comparison table for static pressure of each fan

1	2	3	4	5	6
0,40 in H_2O	0,50 in H_2O	0,11 in H_2O	0,16 in H_2O	0,21 in H_2O	0,26 in H_2O

Figure 1.2 : 5.25” motorized impeller (blower) and a 5.31” tube axial fan

The compared AC and BLDC motors are shown in figure-1.2. The left one of the figure-1.2 is motorized impeller fan and right one is tube-axial fan. Beyond airflow and operating performance at higher static pressures, the advantages of using brushless DC in appliances, or any other application are clearly worth considering:

SPEED CONTROL & NOISE are much easier to control using brushless DC because due to the linear speed torque relationship which means the speed is easily controlled simply by controlling the voltage. Most DC motors operate with the same performance at ±30% voltage. The ability to control speed via voltage provides engineers with an effective means for controlling noise levels, i.e. a speed decrease resulting in a reduced noise level of 3dB lowers the noise level by 50%.

OUTPUT POWER/FRAME SIZE is high for the BLDC motors since they have permanent magnets on the rotor which results in smaller size for a given output power. On the other hand, since stator and rotor have windings in AC induction motors, the output power / frame size is lower.

STARTING CURRENT control is easier in BLDC motors since no special starter circuit is required. However in ac induction machines approximately seven times of rated current is drawn at the starting. It is vital to determine which starter circuit should be selected.

EFFICIENCY, there is no question about the advantage of brushless DC. Pick the wattage rating, or choose any ratio you like, such as CFM per watt, brushless DC is outstanding when compared to AC. Not all brushless DC motors are equal so it is important to compare the efficiencies and performance levels of similar products.

1.2 Single Phase BLDC Motors

The most commonly used BLDC motors are two or three phase permanent magnet ac motors driven by a dc to ac inverter. For instance, three phase BLDC motors require six pulse full bridge inverter to achieve rotational motion with higher copper and iron utilization as shown in figure-1.3. Since these types of BLDC motors are widespread, most of the researches are concentrated on them in the literature. On the other hand, there exist little investigations on structural and operational analysis of single phase BLDC motors. Single-phase motors generally suffer from slower starting torque/speed characteristics, iron and copper losses due to the inefficient utilizations. That is why single-phase BLDC motors come into prominence in low power applications in which rapid response and high efficiency are not so important. The primary advantage of single Phase BLDC motors is that number of components used is reduced because of simple design, which brings an advantage in terms of cost. For

example, when three position sensors and six pulse switching transistors required to be used in three phase BLDC motors, only two switching transistors and one position sensor may become enough for single phase BLDC motors. Moreover, they have advantages in manufacturing by comparing the two or three phase counterparts. These reasons imply that single-phase BLDC motors come forward when cost is more important than the efficiency.

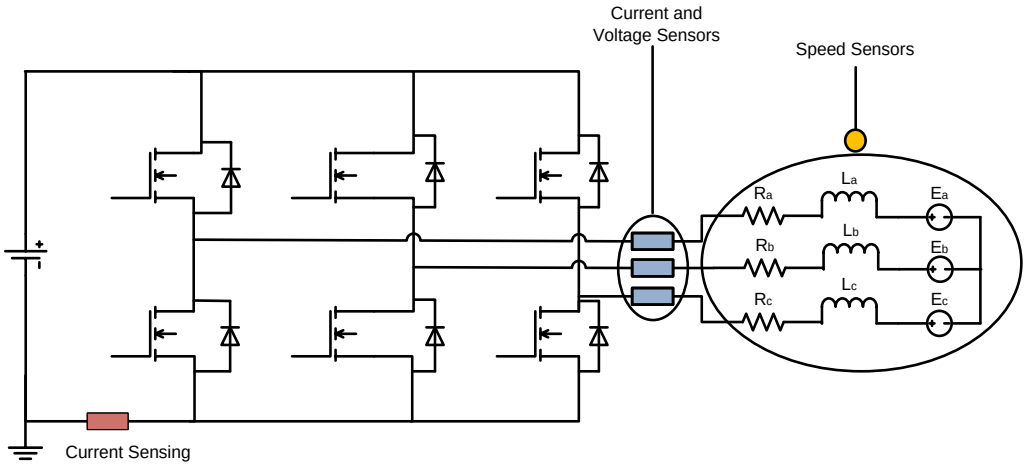

Figure 1.3 : Equivalent circuit of three phase BLDC motor

In this master thesis, a single phase BLDC motor for a fan application with high efficiency and low cost is going to be designed and implemented. It is obvious that every task has its own characteristics. For instance, a compressor requires motors with high torque characteristics with start/stop operation or center-driven winders and machine tool spindles need high torque at low speed and low torque at high speed. However, the priorities of the requirements are very different for a ventilation application. Fan load has a characteristic, which requires low torque at low speed and high torque a high speed. It also shows very small torque fluctuations under continuous operation. Since the designed motor will be used in ventilation fan application, a single-phase BLDC motor becomes a good alternative due to their low starting torque requirements, cost effectiveness, simplicities in manufacturing processes.The single phase BLDC motors are generally driven by a drive circuit, which consists of four switches, connected as H-bridge (figure-1.4). This driving circuit makes the phase winding to be conducted over 180^0 for both positive and negative cycles according to the signals come from the position sensor such as Hall Effect sensors. This driving technique suffers from generating null points in torque waveforms, which makes the single-phase BLDC motors difficult to start up.

For very low power applications, it is common to use uni-polar inverter in order to reduce the cost of the power switching devices (figure-1.5). In this type of BLDC motors, the windings are wrapped in the slots of the stator as two-phase configuration. The uni-polar inverter is consisting of two power-switching devices. It should be noted that this type of inverter has disadvantages due to the insufficient utilization of copper and power density.

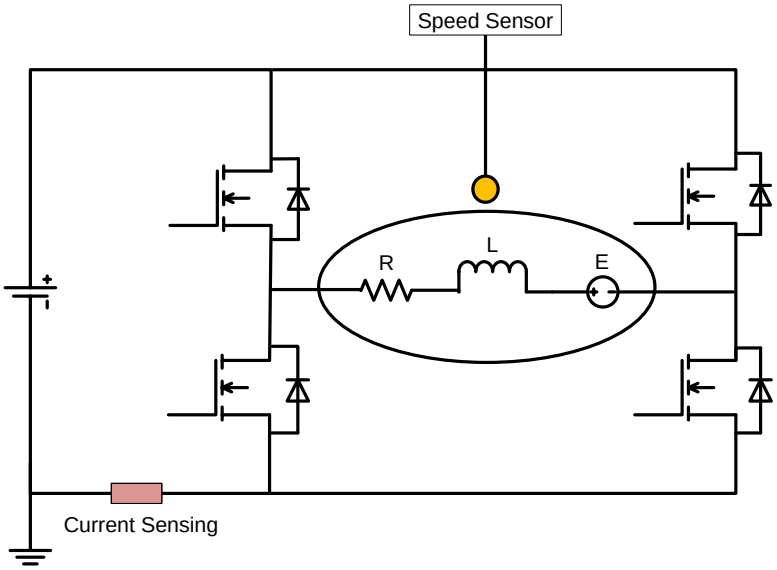

Figure 1.4 : Equivalent circuit of single phase BLDC motor with bi-polar driving

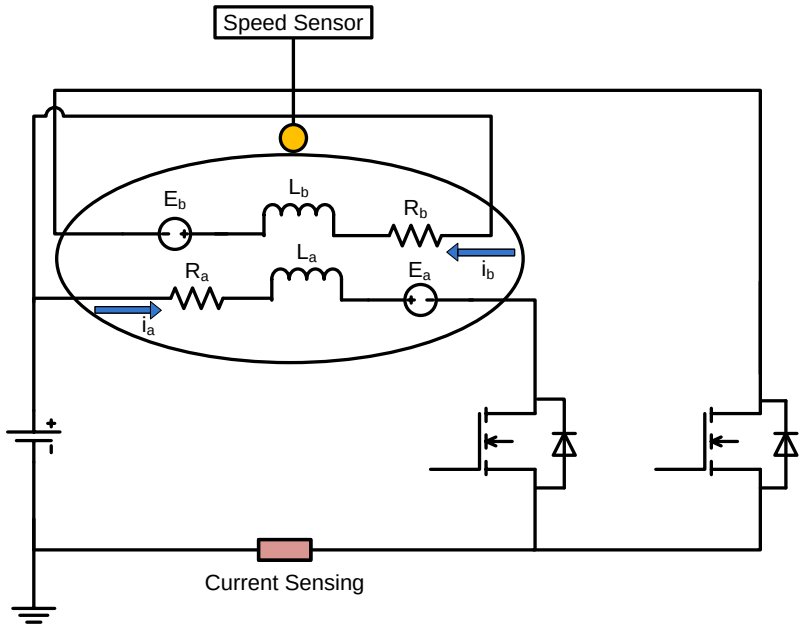

Figure 1.5 : Equivalent circuit of two phase BLDC motor with uni-polar driving

1.3 Literature Review

From beginning of the 1900s, DC motors have been increasingly used in most of the applications due to their easiness of torque and speed control, maintenance-free structure and high moment/current characteristics. However, after the invention of alternating current motors, asynchronous motors have become widespread because of advantages of AC electric transmission over DC transmissions and difficulties related to the collector and brush structures [2]. After developments achieved in power electronics, microcontrollers, DSP control units, permanent magnets (invention of Samarium Cobalt in 1970s and Neodymium Boron magnets in 1980s), researchers and scientists show increasing interests on BLDC motors especially PMBLDC motors. Extensive research attempts have been made in order to reduce the cost and increase efficiency of PMBLDC motors. Several journals and papers have been written about PMBLDC motors by focusing on different aspects of PMBLDC motors such as design and analysis of motors, different structural design of stator and rotor, different drive techniques and etc.

In study [3], design and performance of single-phase and three-phase PMBLDC motors for vacuum cleaners are considered. Universal motors are mostly used in most of the vacuum cleaners because of their low cost. However, their noise levels, high electromagnetic radiations that are unacceptable according to European Directives and inefficiency push the authors to make a research on this area. Firstly, conventional drive technique is shown for universal motor. Then size of the stator and rotor are determined according to the space given in vacuum cleaners. After that, the drive techniques are stated for both single and three phase PMBLDC motors. Structure of the both single and three phase motors are determined by focusing on the torque waveform. Experimental and simulation results are given under four parameters for each type of motor. Firstly, the results are compared in terms of the back EMF and current waveforms of universal motors, single and three phase PMBLDC motors. Secondly, electromagnetic performance of the three type motors are compared and results showed that single and three phase motors have higher efficiency than universal motors and three phase motor have higher power density and efficiency than single phase motors. Thirdly, acoustic noise level are measured and results show that average noise level emitted by universal motor is 8dB higher than three phase PMBLDC motor and 10 dB higher than single phase PMBLDC

motor. Finally, electromagnetic compatibilities are compared and single and three phase PMBLDCM motors emits permissible electromagnetic radiation whereas emission of universal motors are not in the acceptable levels.

A journal paper about PMBLDC motor drives are published in 2009 [4]. This study mentions about the drive techniques for PMBLDC motors by focusing on the sensorless control. Huge literature researches are done by the authors of the paper in order to provide wide perspective on various aspects of PMBLDC motors. The classifications, construction types and different control topologies of PMBLDC motors are examined in details. Advantages and disadvantages of these drive techniques are pointed out by showing voltage, current, torque and speed characteristics. Besides, power quality consideration is discussed for the different control topologies.

S. Ahmed and P. Lefley developed single-phase PMBLDC motor from a novel generic model [5]. In this paper, generic model of a novel single phase PMBLDC motor was discussed in details. The purpose of the authors is to obtain a practical model from generic novel model by considering the factors such as efficient iron utilization, low cogging torque, and high starting torque at any rotor position. After the model is generated, FEM analysis is applied and effective results are obtained. The results show that iron utilization is achieved by using pole shoe design in the structure of stator and rotor even without affecting the back EMF wave shape. They also observed that if the small stator poles and rotor are tapered in such a way that magnet have smoother edges, a continuous torque production is obtained with a flat back EMF.

In study [6], investigation of a single-phase brushless DC motor with bifilar stator winding and asymmetrical stator pole faces and its drive system are considered. Under the scope of this work, single-phase bifilar wound BLDC motor which is designed to be used in computer disc drive spindle is analyzed. Firstly, advantages of single phase BLDC motors over three and two phase ones are stated. Then structure of stator and rotor with magnets are given in details. The diameter of stator and rotor, air gap distance and some unusual slots are mentioned. The schematic diagram of the bifilar winding and current directions are stated. After that, inverter circuit is shown in which there exist two switching transistors and two zener diodes. The inverter switching logic circuit is also discussed in details.

The switching sequence is obtained by use of one hall-effect sensor and required number of logic gates. After the description of the four poles, single phase BLDC motor is completed, the analysis and model of the motor is derived. At first, flux linkage and electromagnetic torque equations are obtained according to two poles BLDC motor then the model is updated by correcting only electromagnetic torque equation, electrical rotor position and velocity according to four pole structures. Experimental and simulation results are compared in terms of steady state and dynamic performance. The results shown are very similar to each other. Especially, authors focus on the starting characteristics in which cogging torque is examined. It is concluded that the cogging torque is intentional result of stator asymmetry and it plays an important role in making the rotor to required position so that sufficient electromagnetic torque is developed to start motor when it is suddenly energized.

A journal paper about determination of torque–speed–current characteristics of a brushless DC motor by utilizing back-EMF of non-energized phase was published in 2006 [7]. In this research, a new method for determining the torque constant and torque & speed characteristics of BLDC motor by the help of back EMF variation of non-energized phase is proposed. In this method, since back EMF is the difference between neutral voltage and supply voltage when no current flows in non-energized coil, authors superimposed a PWM signal and determined the back EMF by measuring period of commutation, max-min values of neutral and terminal voltages. After obtaining back EMF and speed, torque constant is determined by use of back EMF equation. This proposed method is used in the newly developed DSP controller in order to observe the real time current, voltage and speed. The results of the new proposed method are also compared with the results of the experiment in which the torque is measured by a dynamometer. The results show that the proposed method predicts the torque–current–speed characteristics as accurately as the dynamometer. There is ignorable error about less than %2.7 between the results.

1.4 Scope and Outline of the Thesis

In this project, design and implementation of PMBLDC motor for fan application will be considered. Firstly, mechanical parts of the fan are designed by using 3-D design program.

Then both the environment in which the PMBLDC fan motor will work and the mechanical parts are designed and simulated. The torque-speed load characteristic of the fan is derived by both experiment and simulation. Design parameters are obtained according to the simulations and experiment. Magnetic model is determined and effective results are obtained. The outline of the thesis is explained as follows.

In the first section of the thesis, BLDC motor technologies for ventilation applications are discussed in details. Good comparisons between BLDC and AC motors are given in order to imply the important role of BLDC motors in ventilation applications. Then single phase PMBLDC motor is discussed a little. The difference between three phase and single phase PMBLDC is clarified. The reasons why single-phase motor is chosen for the ventilation application and for my thesis are explained. Lastly, literature researches about single-phase PMBLDC motors and design techniques are mentioned briefly.

In the second section of the thesis, theoretical background of BLDC motor is discussed. Firstly, basic relationships related to the magnetic theory are stated very briefly. Then, classifications of BLDC motors are explained in details. Then, different design possibilities for BLDC motors in terms of stator and rotor structures are stated briefly. How a BLDC motor works is explained and related output signal are discussed briefly. Finally, the magnets and sensors used in BLDC motor technologies are considered in details.

In third section, mechanical design is achieved by focusing on the impeller, housing design and the environment in which this fan is going to be used. The impeller and housing are designed and they all simulated in the real environmental conditions to get the optimum design parameters. The torque and speed characteristic of the fan is derived both by experiment and simulation. These results are compared and design parameters are determined for the magnetic design phase.

In the fourth section, magnetic analysis of the motor is achieved and effective results are obtained. The different motor structures are examined in details and simulation results are obtained successfully. These results are compared between themselves and the optimum magnetic design is chosen. The chosen design is compared with mechanical load and satisfactory results are obtained. Final section concludes the thesis with some important remarks.

2. THEORETICAL BACKGROUND of BLDC MOTOR

2.1 Basic Relationships of the Magnetic Theory

Magnetic field is defined by two vector quantities, which are B, and H. B is vector quantity of the magnetic field density that is flowing through a certain area of magnetic material. H is a another vector quantity described as magnetic field intensity due to the interaction of B with the material it encounters as shown in figure-2.1. These two quantities have a collinear relationship in considering the materials used in motors. Actually, these quantities show nearly linear characteristics in a wide operating range even though they have non-linearities in complete characteristics. The relationship between magnetic field density and magnetic field intensity is given in equation 2.1 as shown below.

$$B = \mu H \qquad \textbf{(2.1)}$$

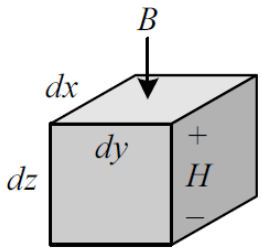

Figure 2.1 : Differential size block of magnetic material.

In equation-2.1, μ is called relative permeability of a material. Relative permeability is a quantity describing degree of the magnetic field that a material can pass through itself. This quantity is given in equation-2.2. The magnitude of μ_0 is equal to $4\pi 10^{-7}$ N/A^2.

$$\mu = \mu_r \mu_0 \qquad \textbf{(2.2)}$$

There exist two fundamental equations used in the analysis of magnetic circuits. First equation describes a relation between magnetic flux and magnetic flux density. The other equation gives relation between magneto-motive force with magnetic field intensity. Each of these equations will be explained briefly.

If a cross section of a magnetic material is exposed to magnetic field density as shown in figure-2.2, the total magnetic flux (Ø) is determined by the two dimensional integral of the magnetic field density and differential area.

$$\emptyset = \int B_z(x,y)\, dxdy \qquad \textbf{(2.3)}$$

If the $B_z(x,y)$ is uniform over a cross section, then the magnetic flux become as given in equation-2.4. The unit of Ø is Tesla (T):

$$\emptyset = BA \qquad \textbf{(2.4)}$$

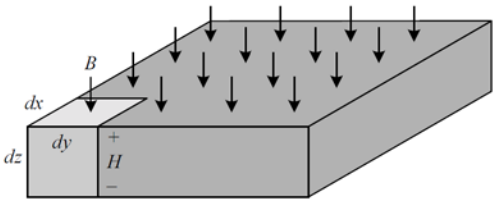

Figure 2.2 : Magnetic material having a differential length.

When a dept is given to the block material in z direction, flowing flux in the successive layers of the material creates change in magnetic field intensity. This change is described by adding the differential effect of magnetic field intensity in z-direction. The relation is given in equation-2.5. The ψ and *l* is defined as magneto motive force and length respectively. The units of ψ, H ans *l* are A/m , A and m respectively.

$$\psi = \int Hdz = Hl \qquad \textbf{(2.5)}$$

As a result of these fundamental equations, permeance is defined as given in equation-2.6. The unit of permeance is Wb/m^2.

$$P = \frac{\mu A}{l} \quad \textbf{(2.6)}$$

Now, it will be useful to mention about the sources of the magnetic field. There are two types of sources creating magnetic field:

- ✓ Magnetic materials (magnets),
- ✓ Electric currents.

Magnet will be discussed in details in the section-2.5. Current cause magnetic field will be discussed here. Oersted found that "an electric current produces a magnetic field." After Oersted's statement, Ampere proposed a relation between current and magnetic field, which is called Ampere's Law. Ampere's law states that the line integral of the magnetic field B around any closed loop it equal to μ_0 times the total net current I_{encl} enclosed by the loop:

$$\oint H.dl = I_{encl} \quad \textbf{(2.7)}$$

When current is carried by N number of wrapped coil, then the total magnetomotive force becomes as,

$$NI = \int Hdz = Hl \quad \textbf{(2.8)}$$

Finally, the force generated on electric current in a magnetic field will be discussed briefly. A magnetic field exerts a force on an electric current. The force on an infinitesimal length of wire dl carrying a current I in a magnetic field B is given in equation-2.9

$$dF = Idl\ x\ B \quad \textbf{(2.9)}$$

If the field B is uniform over a straight length l of wire, then the force is,

$$F = IL\ x\ B = ILBsin(\theta) \quad \textbf{(2.10)}$$

where θ is the angle between magnetic field B and the wire. The direction of the force is perpendicular to the wire and to the magnetic field, and is given by right hand rule. This relation serves as the definition of magnetic field B.

2.2 Classifications of Permanent Magnet BLDC (PMBLDC) Motors

BLDC motors are classified according to the waveform shape of the induced back EMF, namely Brushless Direct Current (BLDC) Motors and Permanent Magnet Synchronous Motors (PMSM). The main differences between the BLDC and PMSM are the shape of back EMF profiles and flux distributions as shown in figure-2.3. For PMSM, the ideal motional EMF is sinusoidal, so that the interaction with sinusoidal currents produces constant torque with very low torque ripple. However, BLDC motors have trapezoidal back EMF waveforms and generated torques with some ripples. They both have excitation windings in the stator and permanent magnets on the rotor [8].

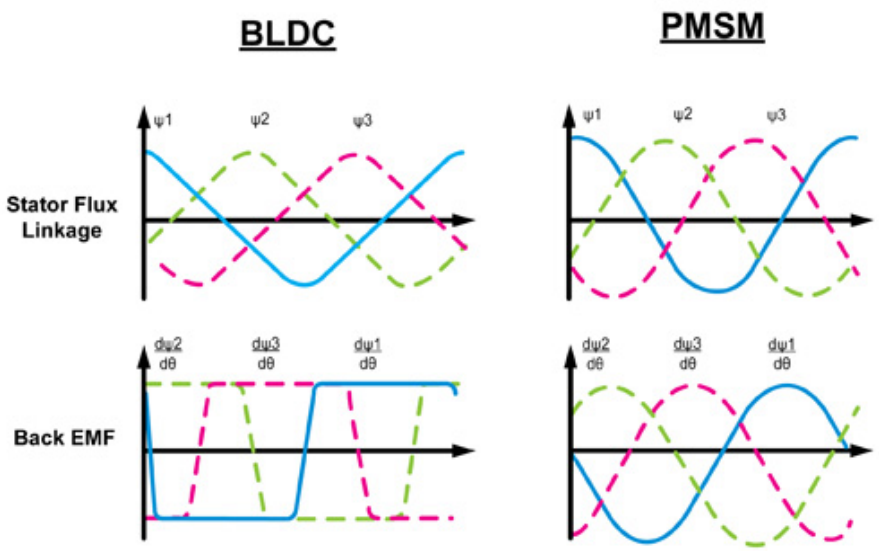

Figure 2.3 : Back EMF waveforms of BLDC and PMSM

The stator windings are distributed with 120^0 angle difference around the air gap in order to create sinusoidal flux change under the magnetic field of magnets on the rotor in PMSM. The excitation phase current is generated in a harmony so that the angular position of the rotor becomes synchronous with phase currents. In these types of motors, driving is achieved by the help of inverter with three current and position sensing components, each of which is used for one phase. It becomes more complicated even when position sensing requires more accuracy.

In BLDC motors, only detecting the commutations in one electrical period for position of rotor and sufficiency of only one current sensing element in the neutral line provide remarkable advantage and easiness in driving. This also will positively affect the cost because of the non-requirement for very precise sensors. Moreover, BLDC motors have their losses on the stator rather than rotor due to its construction. This becomes an advantage since heat is dissipated more easily. They also have high torque characteristics with some ripples as compared to PMSM motors.

Consequently, the PMSM is more efficient and has lower torque ripple than the BLDC motor. Between the two types of PMBL motors, PMSM is, therefore, preferred for applications where accuracy is desired e.g. robotics and numerical controlled machines. The comparison of BLDC and PMSM is also given in table-2.1.

Table 2.1: Comparison of BLDC and PMSM [9]

Comparison of BLDC and PMSM		
	BLDC	**PMSM**
Type of Machine	Synchronous machine	Synchronous machine
Feeding Voltage	Fed with direct currents	Fed with sinusoidal currents
Induce EMF	Trapezoidal Bemf	Sinusoidal Bemf
Flux Variations	Stator Flux position commutation each 60 degrees	Continuous stator flux position variation
Driving	Only two phases ON at the same time	Possible to have three phases ON at the same time
Torque Output	Torque ripple at commutations	No torque ripple at commutations
Harmonics	Low order current harmonics in the audible range	Less harmonics due to sinusoidal excitation
Losses	Higher core losses due to harmonic content and less switching losses.	Lower core loss and higher switching losses at the same switching frequency
Control	Control algorithms are relatively simple	Control algorithms are mathematically intensive

2.3 Constructions of BLDC Motors

2.3.1 Radial flux motors

2.3.1.1 Internal rotor

In internal rotor motors, rotors appear inside the stator as shown in figure-2.4. The windings are placed in the nonmoving stator part and magnets are placed in the rotating part, rotor. Internal rotor construction is commonly used in several applications. This structure provides a natural shielding to rotor and makes the mounting of motor to the surrounding easier. Moreover, internal rotor motors are better suited than external ones in terms of drive functionality. Since the internal rotors have low moment of inertia, reaching fast rotating speeds and quick change of direction are easier in these types of motors.

There exist various types of inner rotor structures available in the literature. Only some of them are shown in Figure-2.4. Every rotor and magnet structure has both advantages and disadvantages. The traditional rotor structure with arc shape magnet is given in figure-2.4a. When magnet is manufactured by the bonding process rather than sintering, it is produced as shown in figure-2.4b. If more flux concentration is desired, then solution may be the magnet shown in figure-2.4c. For higher speed motor applications, the rotor structure in figure-2.4d may be a good alternative since the magnets are embedded inside the rotor so that they become very difficult to brake off.

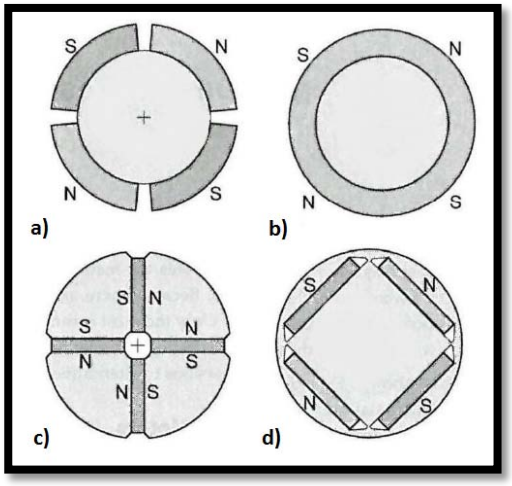

Figure 2.4 : Different types of inner rotor structures [10].

2.3.1.2 External rotor

In external rotor motors, the turning rotor embodies the excitation winding (figure-2.5). High torque and good synchronous operation can be achieved. Since the rotor is easily accessible from the outside, it become well suited for applications such as ventilation fans, cooling applications where embody design is crucial. In a similar way it is now expected that operating noise be almost inaudible and the speed be perfectly controlled. It should be noted that the bearings be protected against shock and vibration.

Since most motor heat is produced in the rotor, making it the rotating element and keeping the stator stationary have several very important effects on performance:

- More effective cooling provides improvements in reliability and the life of the motor,
- Motor efficiency and size/output relationships are better than with induction-type motors. [10]

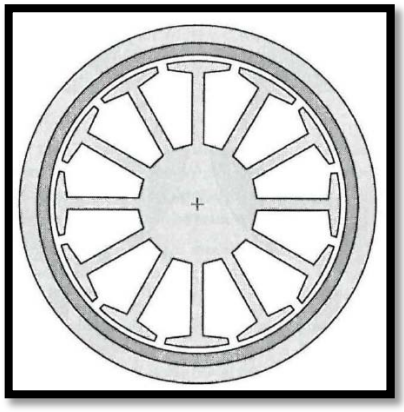

Figure 2.5 : Cross section of an external rotor [10].

Even if the external rotor motors operate at low speeds which in turn increases heat, current (amps) increases only slightly (in many internal rotor motors current often rises 30% to 40%). Superior cooling and heat dissipation from the motor still occurs because the airflow passes over the rotor. Speed control is very easy with external rotor motors by voltage reduction using fixed or variable resistors, autotransformers, or electronic speed controllers. Speed control has better linearity, too. Because motors are totally enclosed, they run clean and stay clean for long life operation. Shorter lamination stacks reduce copper losses. Less induction is required to reach equivalent torque. The operating temperature range for most blowers or fans is

commonly -22°F to + 300°F (-30°C to + 150°C) but varies with motor type and power selection. External rotor motors are also better when multiple motors operate simultaneously in a system at a common frequency or speed, for example, using several fans in a fan tray or fan rack, or using one blower at an intake inlet and another at an exhaust outlet [10].

2.3.2 Axial flux motors

The history of the axial flux motors starts from the invention of the first ac induction machine. Michael Faraday developed the first primitive machine, which has an axial flux construction in 1882. Since then, the developments achieved in the motor technologies push the sector to concentrate more on the radial flux motors due to the difficulties experienced in manufacturing of axial flux motors. These difficulties can be counted as follows. Firstly, the stator construction requires very time-consuming manufacturing process with high cost due to the circumferential lamination. This problem is easily handled by stacking the laminated sheets by stamping machine. Some examples of axial flux motor are shown in figure-2.6.

The rotational motion is achieved by changing the orientation of the windings and magnetic field. The created magnetic field is in the axial direction since the winding are wrapped in the radial direction. This structure is the opposite as compared to the radial flux motors. For the axial flux motor package, construction that is shown in figure-2.6d has more advantages than the other ones shown in figure-2.6a, b, and c. This is because the magnets on the rotor always try to reduce the air gap that results in unbalanced forces.

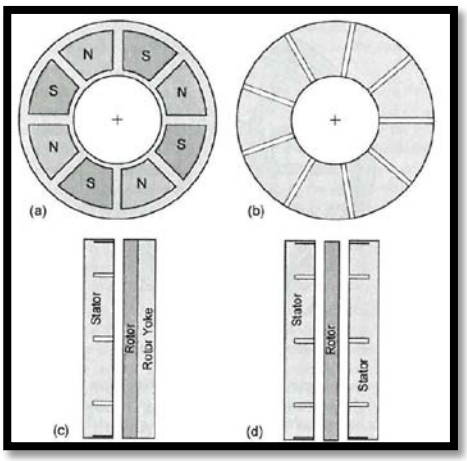

Figure 2.6 : Axial flux motor configurations [10].

2.3.3 Linear motors

Linear motors have been used in several applications for several decades. The main difference is the structural not theoretical since operation is very similar to the rotary motors. A linear motor is essentially a rotary motor that has been cut and made flat. There are several reasons why linear motors are demanded in the market. On e the reasons is that linear motors overcome the most of the disadvantages of the most commonly used ball screws. Since the ball screws are being worn due to the high speed and temperature, these problems limit the success rate of the system. Control of the linear motors is also identical to the control of rotary ones since no mechanical commutators are used.

There are several different constructions related to the linear motors. One type of construction is that magnets are stationary and windings are in the pitches of moving part (rotor). This construction, called “moving coil design” becomes advantageous in short stroke applications (figure-2.7a). In the other type, the construction is vice-versa, windings are on the stator and magnets are on the rotor. This construction called “moving magnet design” comes forward in long stroke application because the increasing cost effect of magnets is reduced by placing them on the rotor (figure-2.7b). Moreover, there exist linear motors in which rotor is sandwiched between two stators (Figure-2.7c, d). This structure offers more holding force for rotor.

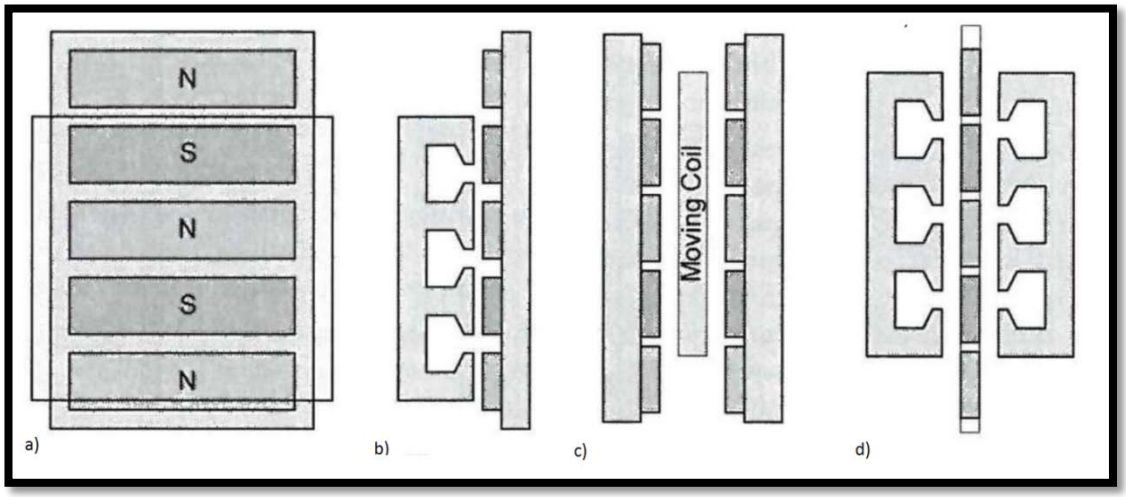

Figure 2.7 : Linear motor configurations [10].

2.4 Principles of Operation of BLDC Motors

In order to explain the how a BLDC motor works, it is more understandable to use three phase structures instead of single phase ones since the three phases BLDC motors involve rules that are more general. The difference between three phase and single phase in terms of principle of operation of BLDC is that only number of phases and components are tripled in three phase ones.

To simplify the explanation of how to operate a three-phase BLDC motor fundamental BLDC with only three coils is considered. To make the motor rotate the coils are energized (or “activated”) in a predefined sequence, making the motor turn in one direction, say clockwise. The motor runs in the opposite direction by running the sequence in reverse order [15].

One should understand that the sequence defines the direction of the current flow in the coils and thereby the magnetic field generated by the individual coils. The direction of the current determines the orientation of the magnetic field generated by the coil. The magnetic field attracts and rejects the permanent magnets of the rotor. By changing the current flow in the coils and thereby the polarity of the magnetic fields at the right moment – and in the right sequence –, the motor rotates. Alternation of the current flow through the coils to make the rotor turn is referred to as commutation.

A three-phase BLDC motor has six states of commutation. When all six states in the commutation sequence have been performed, the sequence is repeated to continue the rotation. The sequence represents a full electrical rotation. For motors with multiple poles, the electrical rotation does not correspond to a mechanical rotation. A four-pole BLDC motor uses two electrical rotation cycles to per mechanical rotation. When specifying the number of Rotations Per Minute subsequently, the number of electrical rotations is referred to unless otherwise mentioned (Figure-2.8).

The most elementary commutation driving method used for BLDC motors is an on-off scheme: A coil is either conducting (in one or the other direction) or not conducting. Connecting the coils to the power and neutral bus induces the current flow (accomplished using a driver stage). This is referred to as square wave commutation or block commutation. An alternative method is to use a sinusoidal type waveform. The block commutation method in going to be covered here. The strength of the magnetic field determines the torque and of the motor. By varying the current flow thought the coils, the speed and torque of the motor can be varied. The most common way to control the current flow is to control the (average) current flow through the coil. This can be accomplished by switching the supply voltage to the coils on and off so that the relation between on and off time defines the average voltage over the coil and thereby the average current.

For BLDC motors, the commutation control is handled by electronics. The simplest way to control the commutation is to commutate according the outputs from a set of position sensors inside the motor. Usually Hall sensors are used. The Hall sensors change their outputs when the commutation should be changed [11].

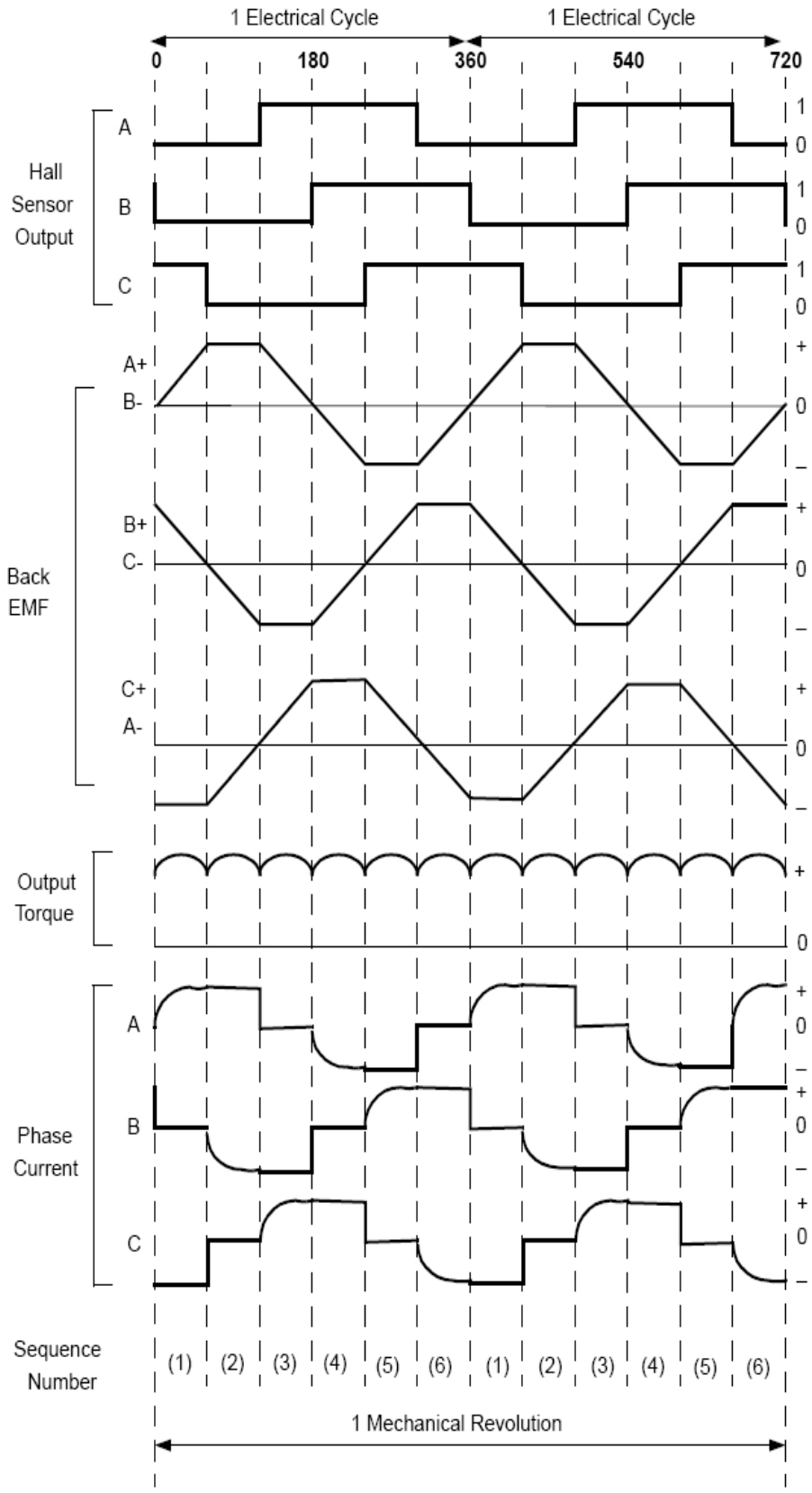

Figure 2.8 : Output and input signal of three-phase BLDC motor [11].

2.5 Permanent Magnets for BLDC Motors

The modern history of permanent magnets has started in 1940s with the invention of Alnico permanent magnets. Before that, a few applications such as magneto or compass are common in the world. A revolutionary development was introduced in 1970s with the invention of Samarium-Cobalt family of hard ferromagnetic materials, which have high magnetic energy densities as compared to Alnico magnets. After later, General Electric and Sumitomo Special Metal Company announced their invention of new type of rare-earth type magnet, namely Neodymium-Iron-Boron (NdFeB). This type of rare-earth magnet does not have only higher magnetic density but also advantageous in terms of cost. Researches concentrated on motors with permanent magnets have gained acceleration with such developments experienced in magnet technologies.

The structure of the field system in PMBLDC motors are closely related to the permanent magnets used in BLDC motors. Every permanent magnet has its own characteristics. A ferromagnetic material gains permanent magnet characteristics when exposed to magnetic field intensity. After this exposure, the domains of the ferromagnetic materials are aligned in the direction of the applied magnetic field intensity. After this exposure is removed, the material is called soft ferromagnetic material if it returns to its initial state due to losing magnetization and on the other hand, it is called hard ferromagnetic material since big fraction of magnetic flux residues in the material. Soft ferromagnetic materials are appropriate to be used as electromagnets whereas hard ferromagnetic materials are to be used as permanent magnets.

Permanent magnets are the magnetic material with large hysteresis loops. After the magnetic field intensity is shut off, some recoiling is happened in the ferromagnetic material. The remanence magnetic flux is denoted by Br. After this demagnetization, the material behaves like the permanent magnet anymore. That is why most of the permanent magnets work in the second quadrant of the BH curves as shown in figure-2.9. In this figure, BH curve for the permanent magnet is shown with blue line.

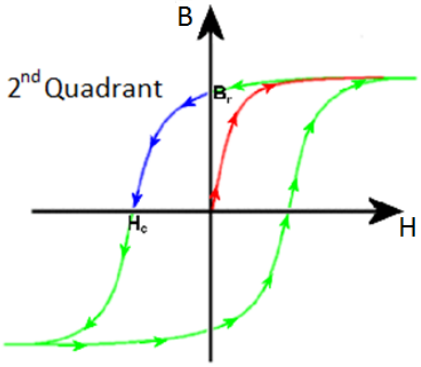

Figure 2.9 : The B-H loop of a permanent magnet.

Temperature is a limiting factor for the applications in which permanent magnets are used (Figure-2.10). For example, NdFeB magnets start to lose its magnetization effect after 75^0C. The amount of lost magnetization is regained after the temperature falls below 75^0C. However, magnets do not gain lost magnetization even after the temperature falls below the limit temperature after passing over the limit temperature. This temperature is known as Cruie temperature.

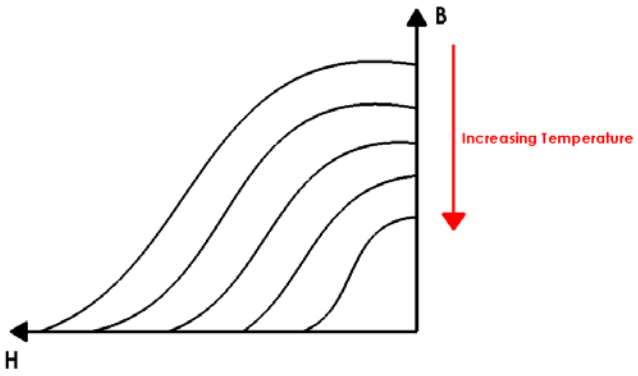

Figure 2.10 : Influence of temperature on the demagnetization curve.

2.5.1 Magnetic Model of Permanent Magnet

The magnetic model of the permanent magnet given in figure-2.11 is derived as shown in equation-2.11

$$\emptyset = \emptyset_r + P_m F_m \qquad \textbf{(2.11)}$$

The fixed field source is given in equation-2.12

$$\emptyset_r = B_r A_m \qquad \textbf{(2.12)}$$

is a fixed flux source, and the permeance of the magnet is given in equation-2.13

$$P_m = \frac{\mu_r \mu_0 A_m}{l_m} \tag{2.13}$$

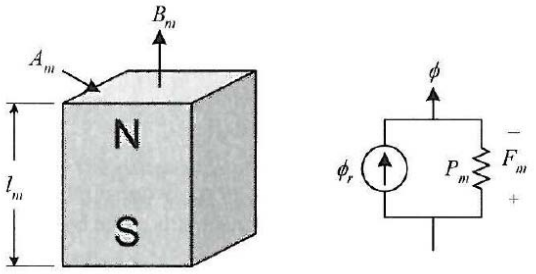

Figure 2.11 : A rectangular magnet and its magnetic circuit model [10].

If the magnet shape is radial as shown in figure-2.12, then the magnetic circuit is derived similar to above equations. The permeance of the radial magnet is given in equation-2.14, (it is assumed that $l_m << r_i$)

$$P_m = \frac{\mu_r \mu_0 L \theta_m r_i}{l_m} \tag{2.14}$$

The flux source is given as in equation-2.15,

$$\emptyset_r = B_r A = B_r L \theta_m r_i \tag{2.15}$$

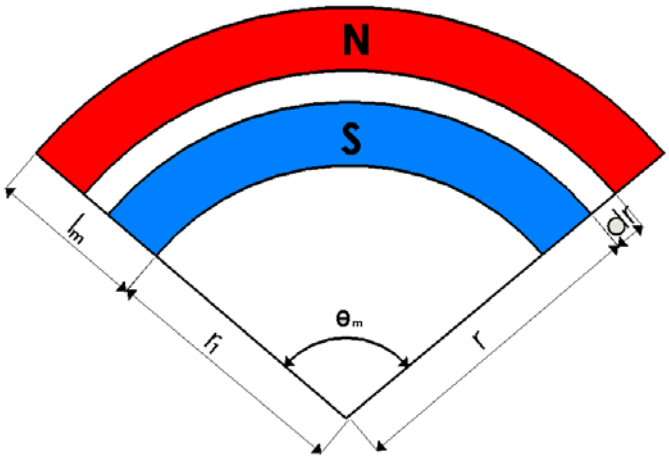

Figure 2.12 : An arc-shaped magnet magnetized radially.

2.5.2 Types of permanent magnets used in BLDC motors

There are four main classes of permanent magnets:

- ✓ Neodymium Iron Boron (NdFeB or NIB)
- ✓ Samarium Cobalt (SmCo)
- ✓ Alnico
- ✓ Ceramic or Ferrite

The magnets can also be classified according to the manufacturing technique;

Injection moldable magnets are composite of resin and magnetic powders of different materials allowing parts to be made in an injection molding process. Energy products are dependent upon the magnetic powders used in fabrication. The molding process allows for the manufacture of more complex shapes. These magnets are usually lower in magnetic strength as there are limitations to the degree of loading.

Flexible magnets are similar to injection-molded magnets, using a flexible resin or binder such as vinyl and produced in flat strips, shapes or sheets. These magnets are lower in magnetic strength but can be very flexible depending on the binder used. Flexible magnets can be used in industrial printers.

Definitions of the common terms that gives information about the characteristics of the permanent magnets;

Br: Is measure of its residual magnetic flux density in Gauss (Tesla), which is the maximum flux the magnet is able to produce.

H_c: Is the measure of the coercive magnetic field strength in Oersted (A/m) or the point at which the magnet becomes demagnetized by an external field.

BH_{max}: Is a term of overall energy density. The higher number, the more powerful the magnet.

T_{coef} of B_r: Is the temperature coefficient of Br in terms of % per degree Centigrade. This tells you how the magnetic flux changes with respect to temperature. -0.20 means that if temperature increases by 100 ^{0}C, its magnetic flux will decrease by 20%.

T_{max}: Is the maximum temperature the magnet should be operated at. After the temperature drops below this value, it will still behave as it did before it reached that temperature (it is recoverable) (^{0}C)

T_{curie}: Is the Curie temperature at which magnet will became demagnetized. After the temperature drops below this valve, it will not behave as it did before it reached that temperature. If the magnet is healed between T_{max} and T_{curie}, it will recover somewhat, but not fully (it is recoverable) (^{o}C).

2.5.3 Neodymium iron boron (NdFeB or NIB):

Neodymium magnet (also known as Nd Fe B,NIB, or Neo magnet), the most widely used type of rare-earth magnet is a permanent magnet made from an alloy of neodymium, iron, and boron to form the Nd2 Fe12 B tetragonal crystalline structure. Developed in 1982 by "General Motors" and "Surritomo Special Metals", neodymium magnets are the strongest type of magnet made and they are difficult to demagnetize. Max energy products (BH_{max}) reach to 50 MGOe.

These magnets have a higher magnetic strength but are easily oxidized and lower temperature resistance. Surface treatment is developed to increase corrosion resistance.

2.5.4 Samarium cobalt:

Samarium Cobalt magnet, a type of care earth magnet made of on alloy of Samarium and cobalt. They were developed in 1970s. They are generally the second-strongest type of magnet made, less strong than neodymium magnets, but have higher temperature ratings and higher coercivity.They are brittle and prone to cracking and chipping. Samarium-Cobalt magnets have maximum energy products (BH_{max}) that range from 16 MegaGauss-Oersted (MGOe) to 32 MGOe; their theoretical limit is 34 MGOe. They are available in two series namely Series 1:5 and Series 2:17 Series 1:5 magnets ($SmCo_5$) have the energy product ranges from 16:MGOe to 25 MGOe and generally have a reversible temperature coefficient of -0.05%/^{0}C. They have a very high coercivity that is they are not easily demagnetized.

Series 2:17 magnets (Sm_2Co_{17}) have the energy product ranges from 20 MGOe to 32 MGOe. These alloys have the best temperature coefficient of all rare-earth alloys, typically being -0,03%/^{0}C.

2.5.5 Alnico:

Alnico magnets are made of a composite of aluminum, nickel and cobalt with small amounts of other elements added to enhance the properties of the magnet. Before the development of rare-earth magnets in 1970s, they were the strongest type of magnet. Other trade names for alloy in this family are Alni, Alcomax, Hycomax, Columax, and Ticonal. The composition of alnico alloys is typically 8-12% Al, 15-26 % Ni, 5-24% Co , up to 6 %Cu , up to 1 %Ti and the balance is Fe.

Alnico magnets produce magnetic field strength at their poles as high as 1500 Gauss (0,15 Tesla) or about 3000 times the strength of Earth's magnetic field. Some brands of alnico are isotropic and can be efficiently magnetized in my direction. Other types, such as alnico 5 and alnico 8, are anisotropic, with each having a preferred direction of magnetization, or orientation. Anisotropic alloys generally have greater magnetic capacity in a preferred orientation that isotropic type. Alnico's remanence (Br) may exceed 12000 G (1.2 T), its coercivity (H_c) can be up to 1000 Oersted (80 k A/m) its energy product (BH_{max}) can be up to 5.5 MGOe (44 T.A/m). This means alnico can produce a strong magnetic flux in closed magnetic circuits, but has relatively small resistance against demagnetization.

Alnico alloys have some of the highest Curie temperatures of any magnetic materials, around 800^{0}C although the maximum working temperature is normally limited to around 538^{0}C.

Alnico magnets are produced we produced by casting and sintering processes. Sintering offers superior mechanical characteristics whereas casting delivers higher energy products (up to 5.5 MGOe) and allows for design of intricate shapes.

2.5.6 Ceramic (Ferrite):

Ceramic, also known as Ferrite, magnets are made of a composite of iron oxide and barium or strontium carbonate. These materials are readily available and a lower cost than other types of materials used in permanent magnet making if desirable due to lower cost. Ceramic magnets are made using pressing and sintering. These magnets are brittle and require diamond wheels if grinding is necessary. These magnets are also made in different grades. Ceramic -1 is an isotropic grade with equal magnetic properties in all directions. Ceramic grades 5 and 8 are anisotropic grades. Anisotropic magnets are magnetized in the direction of pressing. The anisotropic method delivers the highest energy product among ceramic magnets at values up to 3.5 MGOe. Ceramic magnets have good balance of magnetic strength, resistance to demagnetizing and economy. They are the most widely used magnets today.

Ferrits can also be soft and hard ferrites according to magnetic properties:

Soft Ferrites: Ferrites that are used in transformers or electromagnetic cures contain nickel, zinc, and/or manganese compounds. They have a low coercivity and are called “soft ferrites” The low coercivity means the material’s magnetization can easily reverse direction without dissipating much energy (hysteresis losses), while the material’s high resistivity presents eddy currents in the core, another source of energy loss. Because of their comparatively low losses at high frequency, these are extensively used in the cores of RF transformers and inductors in applications such as SMPS.

Hard Ferrites: In contrast, permanent ferrite magnets are made of hard ferrites, which have a high coercivity and high remanence after magnetization. These are composed of iron and barium or strontium oxide. They also conduct magnetic flux well and have a high magnetic permeability. This enables these so-called ceramic magnets to stone stronger magnetic fields than iron itself. They are cheap, and are widely used in household products such as refrigerator magnets. The max magnetic field is about 0.35 Tesla and the magnetic field strength H is about 30 to 60 kA/m.

The properties of the magnets are given in table-2.2 with the characteristic properites.

Table 2.2: Comparison table of permanent magnets:

Type of Magnet	B_r (Tesla)	H_c (kA/m)	BH_{max} (kj/m^3)	T_{coef}	T_{max}	T_{curie}
$Nd_2Fe_{14}B$ (Sintered)	1.0 – 1.4	750 – 2000	200-440	-0,12	150	310 – 400
$Nd_2Fe_{14}B$ (Bonded)	0.6 – 0.7	600 – 1200	60 – 100	-0,12	150	310 – 400
$SmCo_5$ (Sintered)	0.8 – 1.1	600 – 2000	120 – 200	-0,04	300	720
Sm (Co, Fe, Cu, $Zr)_7$ (Sintered)	0.9 – 1.15	450 – 1300	150 – 240	-0,04	300	800
Alnico (Sintered)	0.6 – 1.4	275	10 – 88	-0,02	540	700 – 860
Sr-Ferrite (Sintered)	0.2 – 0.4	100 - 300	10 - 40	-0,2	300	450

2.6 Sensors for BLDC Motors

BLDC motors need to detect the rotor position in order to determine which winding should be energized at a time. Mainly two alternatives such as with sensors or sensorless options are offered to bring solution to this problem. Since the developments are achieved in microelectronics and integrated circuits, importance of sensorless solutions start to decrease. Even tiny sensors are possible to be manufactured with today's technology with lower cost. Sensorless solutions become alternatives when it is impossible to place a sensor inside the motor construction. For the solutions with sensors, the detection of rotor position is achieved by position sensors such as Hall Effect sensors, encoders and resolvers. Every sensor has its own advantages and disadvantages. Some factors such as linearity, sensitivity, size, type of input/output signals become dominant in choosing which sensor is appropriate for the desired applications. In the following lines, three commonly used position sensor will be discussed briefly.

2.6.1 Hall-Effect sensors

Dr. Edwin Hall discovered the Hall Effect in 1879 while he was studying for his Ph.D. education at Johns Hopkins University in Baltimore. The experiments were successful but no applications outside of the realm of theoretical physics were found for over 70 years. However, with advent of semiconductor materials in the 1950s, applications in which Hall Effect theory is used became widespread. After a while, the Hall Effect theory becomes possible to be applied in a solid-state package, which is easier to be produced in mass production with low cost [12].

The theory of the Hall Effect sensor is based on the interaction of a current passing through a semiconducting sheet material with the externally applied magnetic field. When the hall element is exposed to the magnetic field, the uniformly passing current is disturbed by the Lorentz force. Because of this interaction, a voltage is induced in the terminal of the output (figure-2.13). Under the certain temperature, the induced voltage is expressed by equaiton-2.16.

$$V_H = hI\ x\ B \qquad \textbf{(2.16)}$$

In this equation the h is the sensitivity constant of the hall material, I is the current passing through the hall element and B is applied magnetic field. All of three terms namely, applied magnetic field, induced voltage, and current are perpendicular to each other. Hall Effect sensors are widely used in BLDC motors in different locations according to the structure of the motor with lower cost. On the other hand, the disadvantages of the Hall Effect sensors can be counted as vulnerability to temperature, lower resolution, and space requirements. Some different types of Hall Effect sensor are shown in figure-2.14.

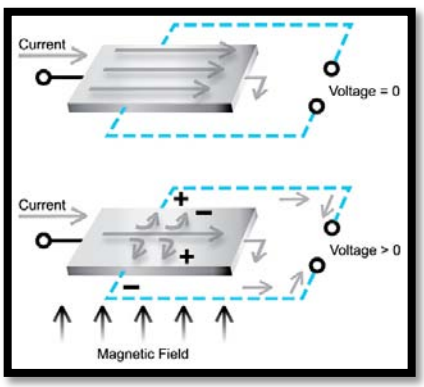

Figure 2.13 : Principle of Hall Effect

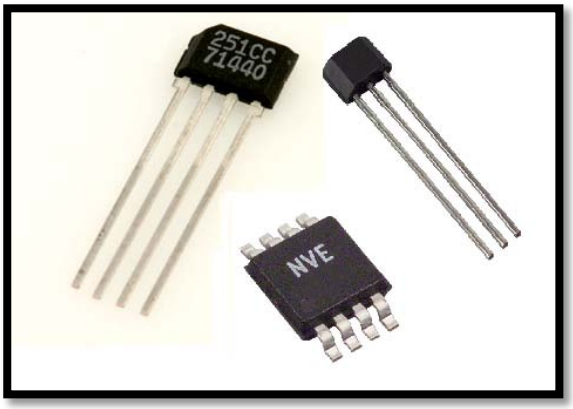

Figure 2.14 : Different type of Hall Effect Sensors

2.6.2 Encoders

An encoder is an electromechanical device that converts linear or rotary displacement into digital or pulse signals. The most popular type of encoder is the optical encoder, which consists of a rotating disk, a light source, and a photo detector (light sensor). The disk, which is mounted on the rotating shaft, has patterns of opaque and transparent sectors electronically coded into the disk (figure-2.15). As the disk rotates, these patterns interrupt the light emitted onto the photo detector, generating a digital or pulse signal output.

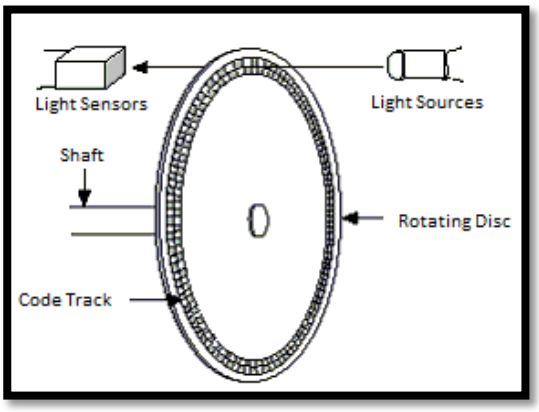

Figure 2.15 : General structure of an encoder

An incremental encoder generates a pulse for each incremental step in its rotation. Although the incremental encoder does not output absolute position, it can provide high resolution at an acceptable price. For example, an incremental encoder with a single code track, referred to as a tachometer encoder, generates a pulse signal whose frequency indicates the velocity of displacement. However, the output of the single-

channel encoder does not indicate direction. To determine direction, a two-channel, or quadrature, encoder uses two detectors and two code tracks.

Encoders are widely used in industrial applications due to their high resolution (until 26 bit single turn), excellent angular accuracy, operating in extreme environments, and high reliability. The only limiting conditions are their high cost and low mechanical strength (Figure-2.16).

Figure 2.16 : A typical application of an encoder with BLDC

2.6.3 Resolvers

A resolver is a position sensor or transducer, which measures the instantaneous angular position of the rotating shaft to which it is attached. The word resolver is a generic term for such devices derived from the fact that at their most basic level they operate by resolving the mechanical angle of their rotor into its orthogonal or Cartesian (X and Y) components. From a geometric perspective, it is similar to the relationship between the rotor angle (θ) and its X and Y components of a right triangle [13].

Fundamentally, then, all resolvers produce signals proportional to the sine and cosine of their rotor angle. Since every angle has a unique combination of sine and cosine values, a resolver provides absolute position information within one revolution (360°) of its rotor. This absolute (as opposed to incremental) position capability is one of the resolver's main advantages over incremental encoders (Figure-2.17).

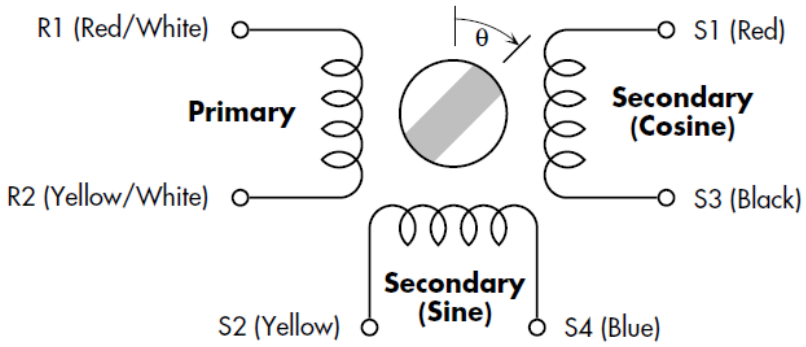

Figure 2.17 : General structure of an resolver

The resolvers have several advantages over the previously mentioned sensors. They have robust mechanical structure, which withstands severe environmental conditions such as oil, low and high temperature, shock and radiation. The output signal is isolated due to the natural transformer structure, which results in natural shielding for the electrical interference. Despite the advantages of mentioned previously, they are not used in BLDC motors as widely as Hall Effect sensors or encoders because of their high cost (Figure-2.18).

Figure 2.18 : Different type of resolvers

3. MECHANICAL DESIGN of the SINGLE PHASE PERMANENT MAGNET BLDC MOTOR

In this section, the design parameters of single-phase PMBLDC motor will be determined. Since this motor is going to be used for ventilation purposes, the design parameters will be determined according to the criteria that give high ventilation efficiency in the environment it is being used.

It is well known that every system has its natural characteristics. It is very vital to know environmental conditions in which the product that is going to be used before delving into the detailed design. In the first part, the environment in which the designed PMBLDC motor is used will be explained. This environment is modeled in 3D program in order to create the real environment. In the second part, mechanical design of the crucial mechanical parts will be discusses in terms of ventilation efficiency. Then the torque & speed characteristic of the system will be derived by experimentally and computer simulation (FEM). Finally, the design parameters for magnetic design will be given in details.

3.1 Environment in which the PMBLDC motor fan is used

This PMBLDC fan is mostly going to be used in the ventilation of computer servers in order to extract the heat from the inside of the server to outside. There exist many computers that radiate heat during the operational time inside a server chassis. The heat must be evacuated continuously in order to provide an efficient working condition for the computers inside the server chassis.

The server chassis with heat sources and fan are modeled by using 3D program, which is shown in figure-3.1. This modeling is very important because it helps us to see which type of impeller, housing and PMBLDC motor should be designed. This modeling gives us a good starting point for the PMBLDC motor in terms of load characteristics, speed and supply voltage.

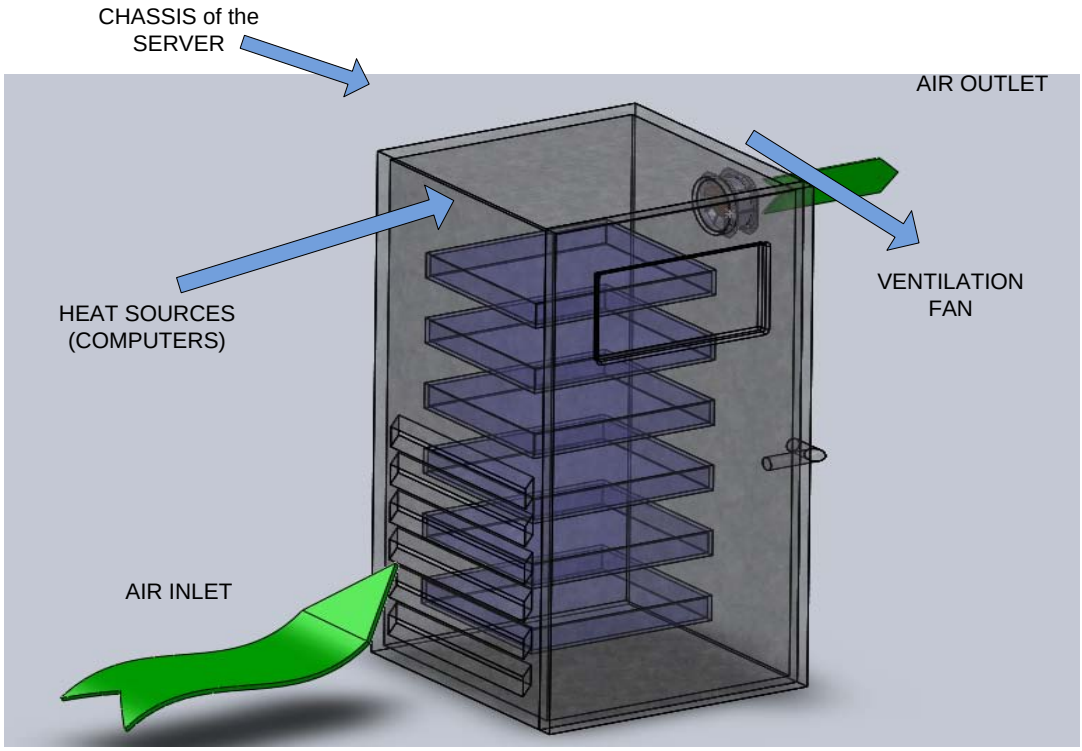

Figure 3.1 : General model of server chassis with ventilation fan

3.2 Mechanical Design of Body and Impellers of Fan(Load)

The main mechanical parts (housing and impeller) of the fan are designed according to the ventilation efficiency achieved in the cooling application of server chassis. The target properties of the mechanical parts are given in the table-3.1.

Table 3.1: Target properties of the mechanical parts

Air Speed	8 m/s – 10 m/s
Impeller Diameter	Ø180mm – Ø220 mm
Housing Diameter	Ø185mm – Ø225mm

The values in table 3.1 are determined according to the acoustic level and space occupied by the fan. The acoustic level increases and becomes very disturbing when the flow speed passes over the 10 m/s. That is why more than 10 m/s is not desired for these type of applications. The mechanical limitations are determined according to physical dimensions of the server chassis in which these fans are going to be used.

The critical step is the design of the impeller since the air movement is directly achieved by this rotating part. The shape, size and even surface areas of the wings definitely affect the ventilation efficiency. This will indirectly affect the torque & speed characteristic of the load according to which the PMBLDC motor is going to be designed.

The housing is designed by considering criteria such as the robust mechanical strength, optimum air passage, minimum vibration, easiness in mounting and manufacturing.

Design-1: Impeller Ø190 mm with 9 blades (Figure-3.2)

Housing Ø200 mm with entrance fillet 10 mm (Figure-3.3)

Design-2: Impeller Ø190 mm with 10 blades (Figure-3.4)

Housing Ø200 mm with entrance fillet 10 mm (Figure-3.3)

Design-3: Impeller Ø200 mm with 11 blades (Figure-3.5)

Housing Ø210 mm with entrance fillet 12 mm (Figure-3.6)

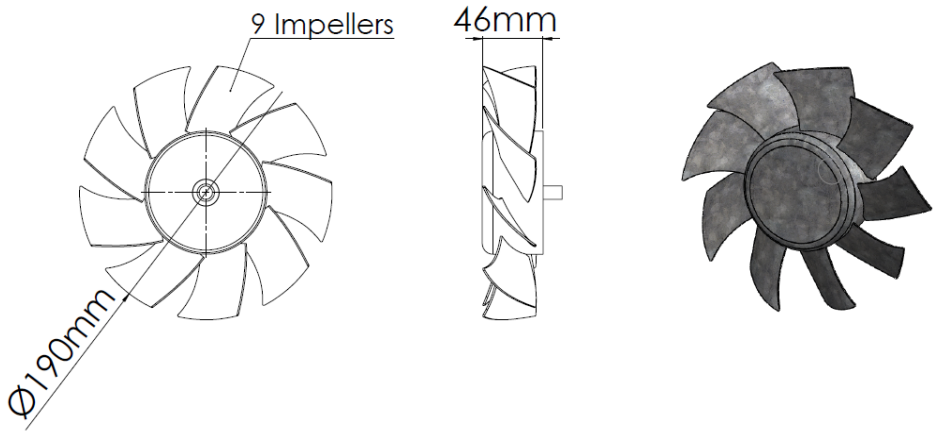

Figure 3.2 : Design-1-dimensions of the impeller

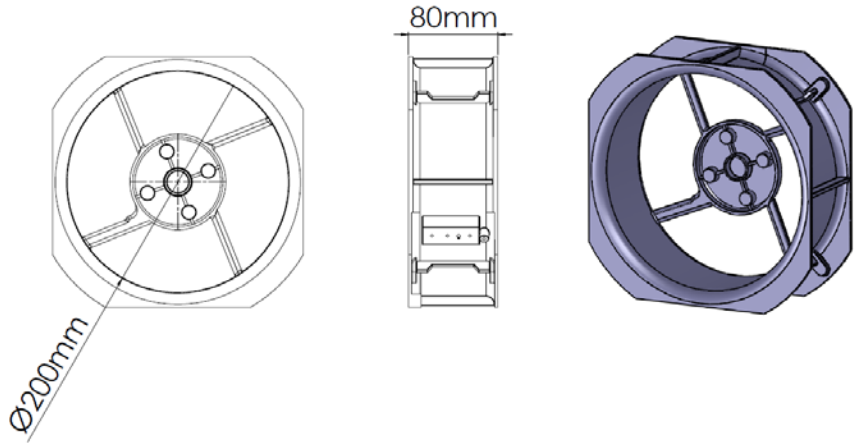

Figure 3.3 : Design-1 & 2 - dimensions of the housing

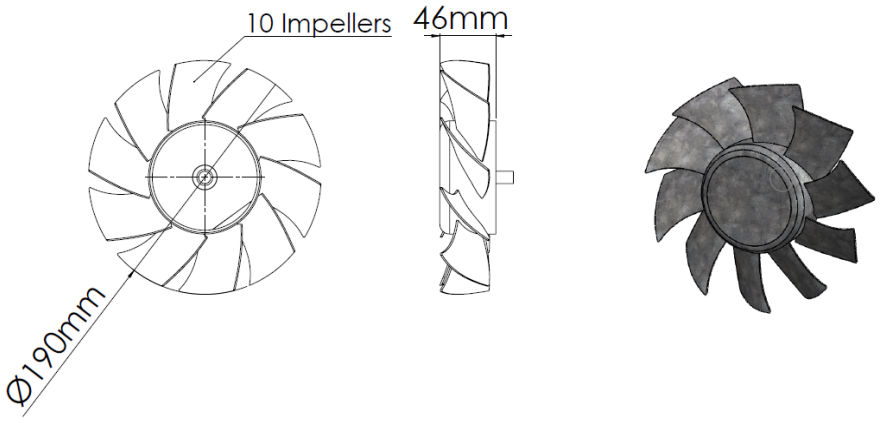

Figure 3.4 : Design-2-dimensions of the impeller

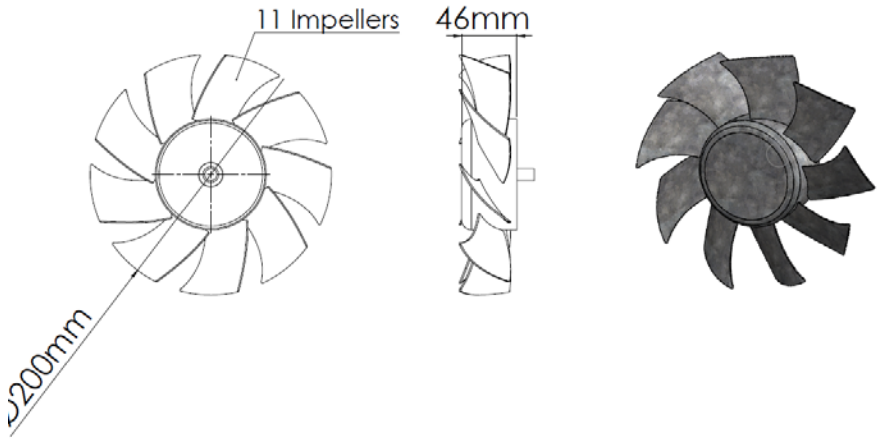

Figure 3.5 : Design-3-dimensions of the impeller

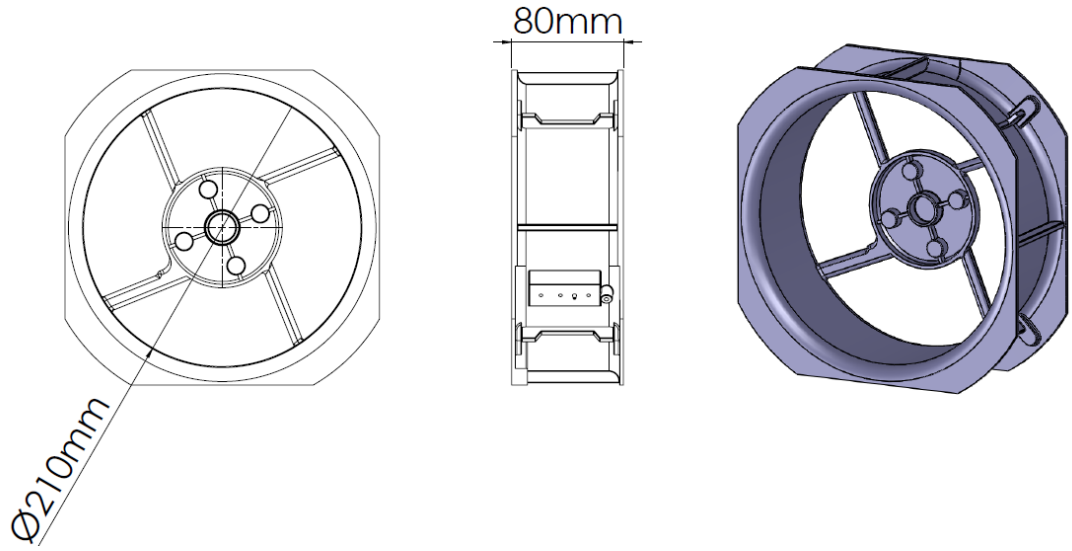

Figure 3.6 : Design-3 - dimensions of the housing

3.3 Results of the Mechanical designs of Impeller and Housing

The impeller and housing are designed according the flow results given in the following figures. The effectiveness of the result will be discussed in details as follows.

3.3.1 Results of design-1

According to the design-1, the results are obtained from figure-3.7 to figure-3.10. Figure-3.7 & 3.8 shows the velocity profile of the fan with 9 impellers. The angular velocity is 308 rad/sec. The flow rate is about 850 m^3/h. The details are given in table-3.2. Figure-3.9 shows the velocity profile of the fan in the server chassis. Figure-3.10 shows the temperature distribution of the server with surface plot. The heat sources (computers) are considered as 100 watt heat sources. As it seen from the temperature scale, the temperature in the server chassis never reaches to the value of 30^0C.

Table 3.2: Results of design-1

	Unit	Value	Averaged Value	Minimum Value	Maximum Value
Outlet_pressure	[Pa]	101315,87	101313,8042	101295,1379	101338,88
Inlet_pressure	[Pa]	101298,44	101299,8159	101247,8442	101332,93
Torque_X	[N*m]	-0,168	0,108	-0,168	0,365
Torque_Y	[N*m]	-0,144	-0,029	-0,145	0,081
Torque_Z	[N*m]	0,091	0,075	0,055	0,113
Flow_rate	[m^3/s]	-0,027	-0,024	-0,0708	0,233
Head	[Pa]	17,43	13,99	-34,86	63,61
Efficiency	[ ]	-0,011	0,018	-0,557	0,78

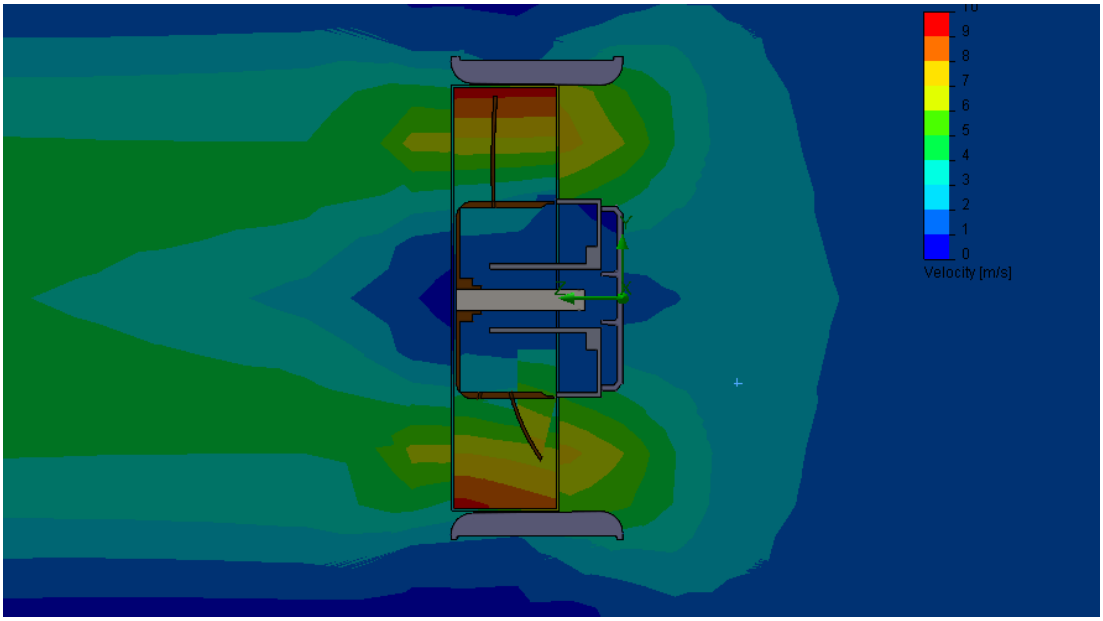

Figure 3.7 : Design-1- Velocity profile of the fan (side view)

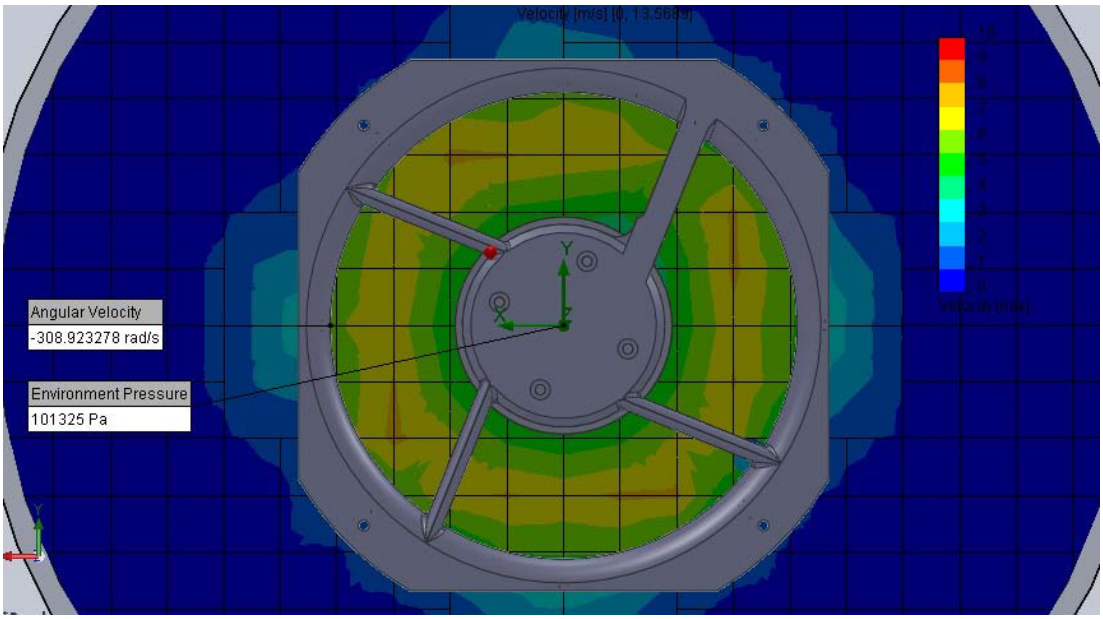

Figure 3.8 : Design-1-velocity profile of the fan (axial view)

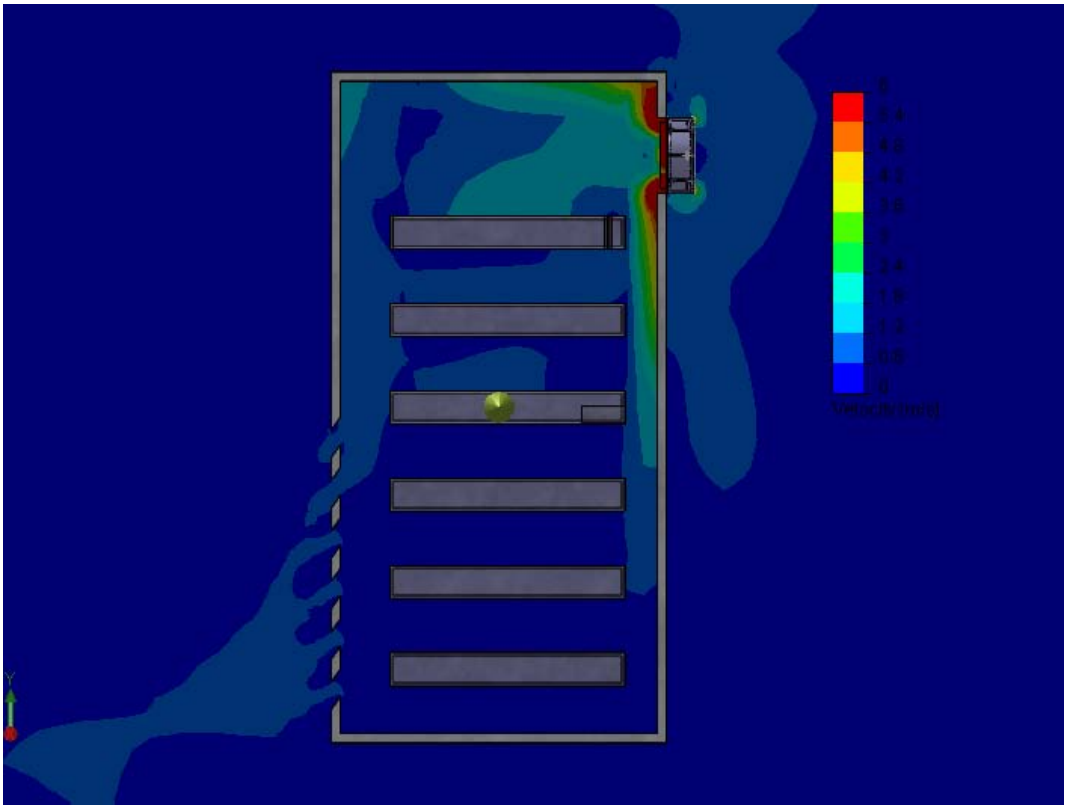

Figure 3.9 : Design-1-velocity profile of the air flow of ventilation fan inside the server

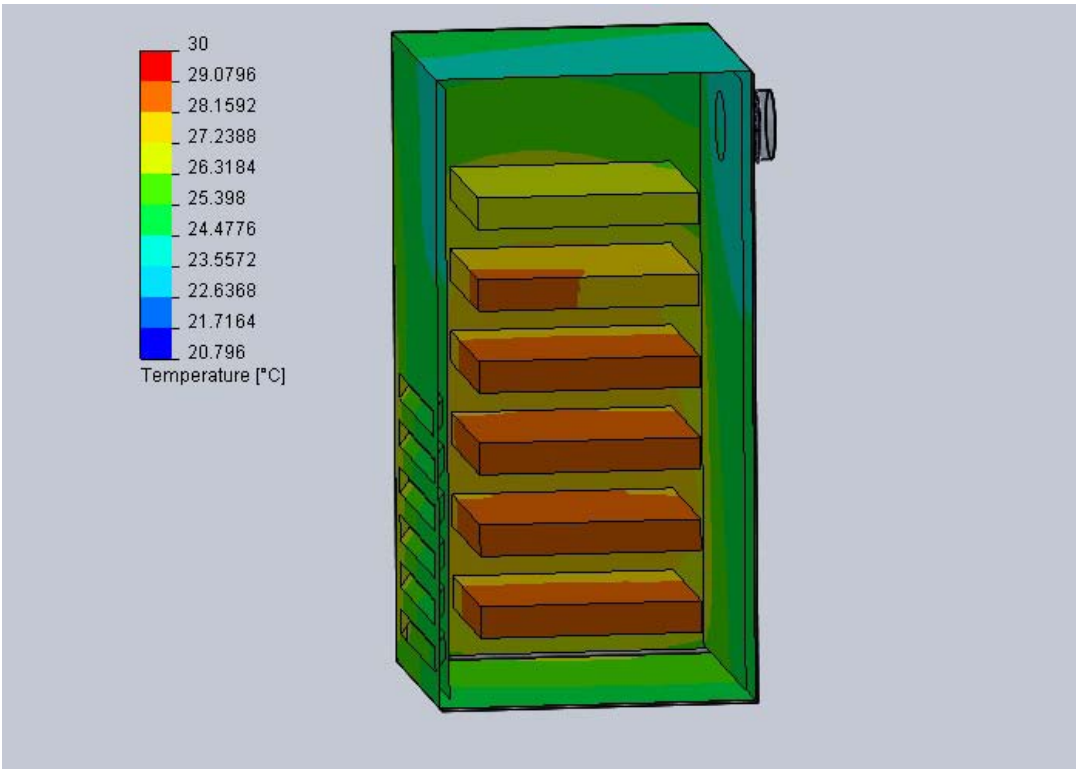

Figure 3.10 : Design-1-temperature distribution of the server with surface plot

3.3.2 Results of design-2

According to the design-2, the results are obtained shown in figure-3.11 and figure-3.12. The angular velocity is 308 rad/sec. The flow rate is about 870 m^3/h. The details are shown in table-3.3. Figure-3.11 shows the velocity profile of the fan in the server chassis. Figure-3.12 shows the temperature distribution of the server with surface plot. The heat sources (computers) are considered as 100 watt heat sources as before. As it seen from the temperature scale, the temperature distribution in the server chassis is does not change enough even though flow rate increases.

Table 3.3: Results of design-2

Goal Name	Unit	Value	Averaged Value	Minimum Value	Maximum Value
Outlet_pressure	[Pa]	101311,83	101312,60	101285,83	101351,56
Inlet_pressure	[Pa]	101257,88	101263,85	101217,17	101311,12
Torque_X	[N*m]	1,13	0,88	0,28	1,43
Torque_Y	[N*m]	0,31	0,34	0,07	0,63
Torque_Z	[N*m]	0,07	-0,01	-0,19	0,10
Flow_rate	[m^3/s]	-0,01	0,06	-0,04	0,28
Head	[Pa]	53,95	48,75	2,96	100,22
Efficiency	[ ]	0,01	-0,02	-0,15	0,30

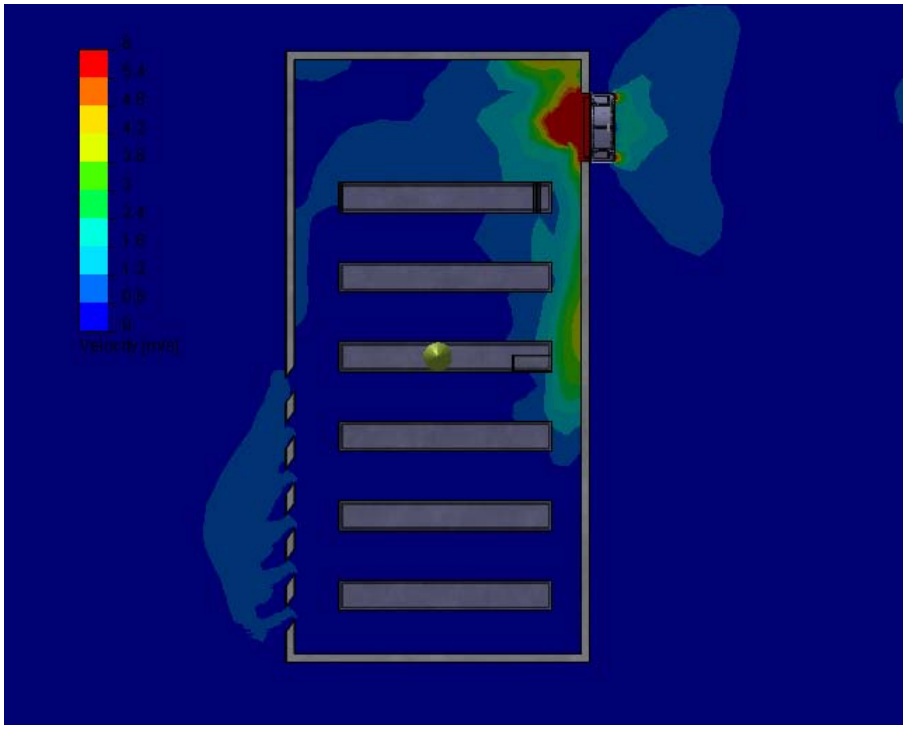

Figure 3.11 : Design-2-velocity profile of the air flow of ventilation fan inside the server

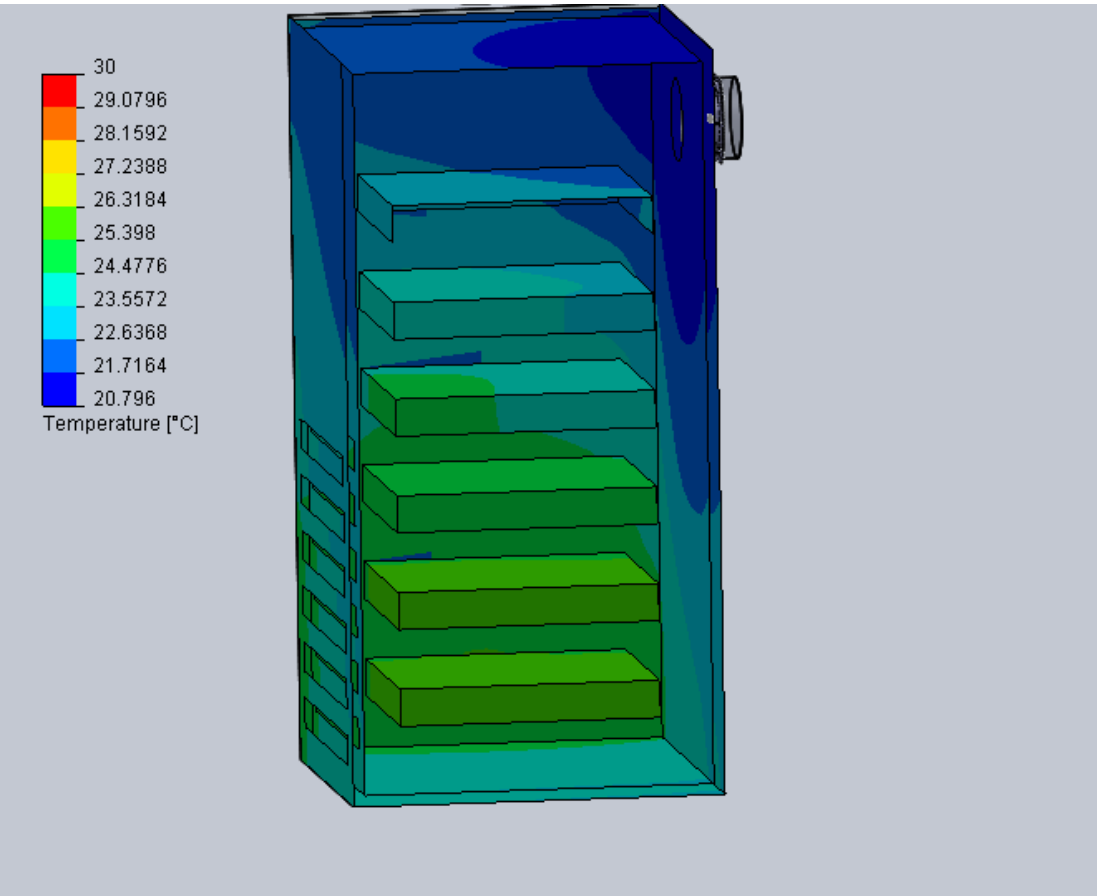

Figure 3.12 : Design-2-temperature distribution of the server with surface plot

3.3.3 Results of design-3

According to the design-3, the results are obtained as shown in figure-3.13 and figure-3.14. This time not only the impeller number is increased but also the diameter of the impeller and housing are increased. The angular velocity is still 308 rad/sec. The flow rate is about 1000 m^3/h. The details are shown in table-3.3. Figure-3.13 shows the velocity profile of the fan in the server chassis. Figure-3.14 shows the temperature distribution of the server with surface plot. The heat sources (computers) are considered as 100 watt heat sources same as previous design. As it seen from the temperature distribution, very effective ventilation is achieved with design-3 comparing by previous designs.

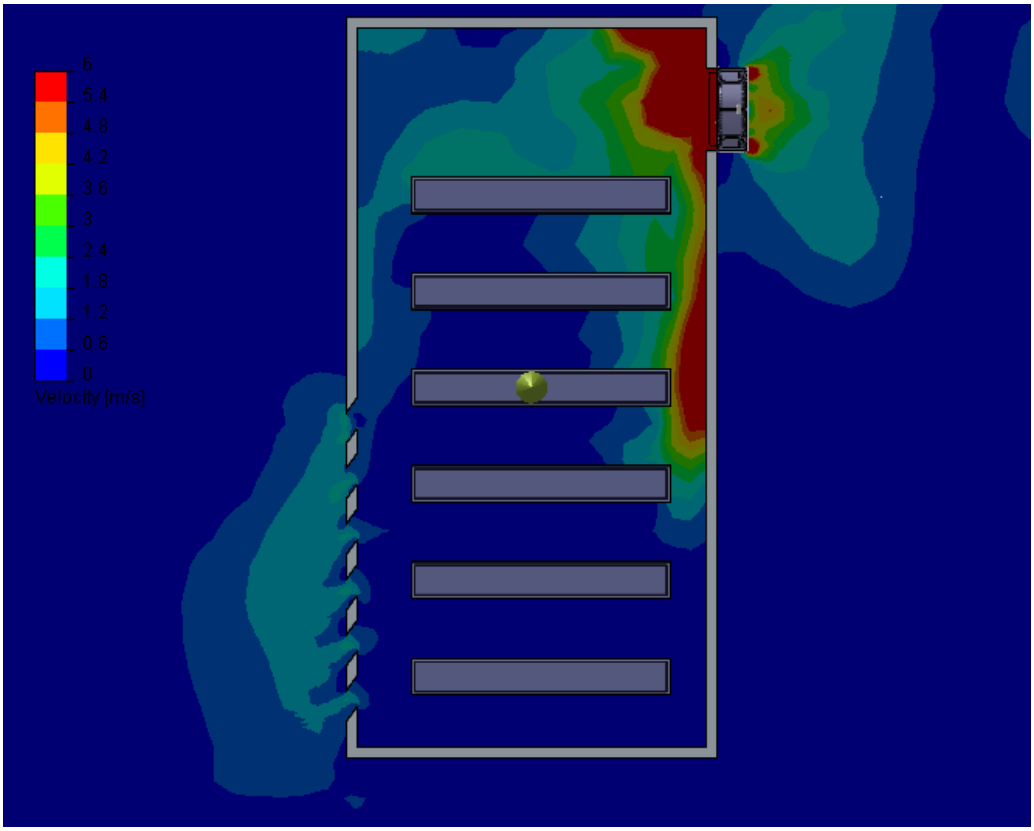

Figure 3.13 : Design-3-velocity profile of the air flow of ventilation fan inside the server

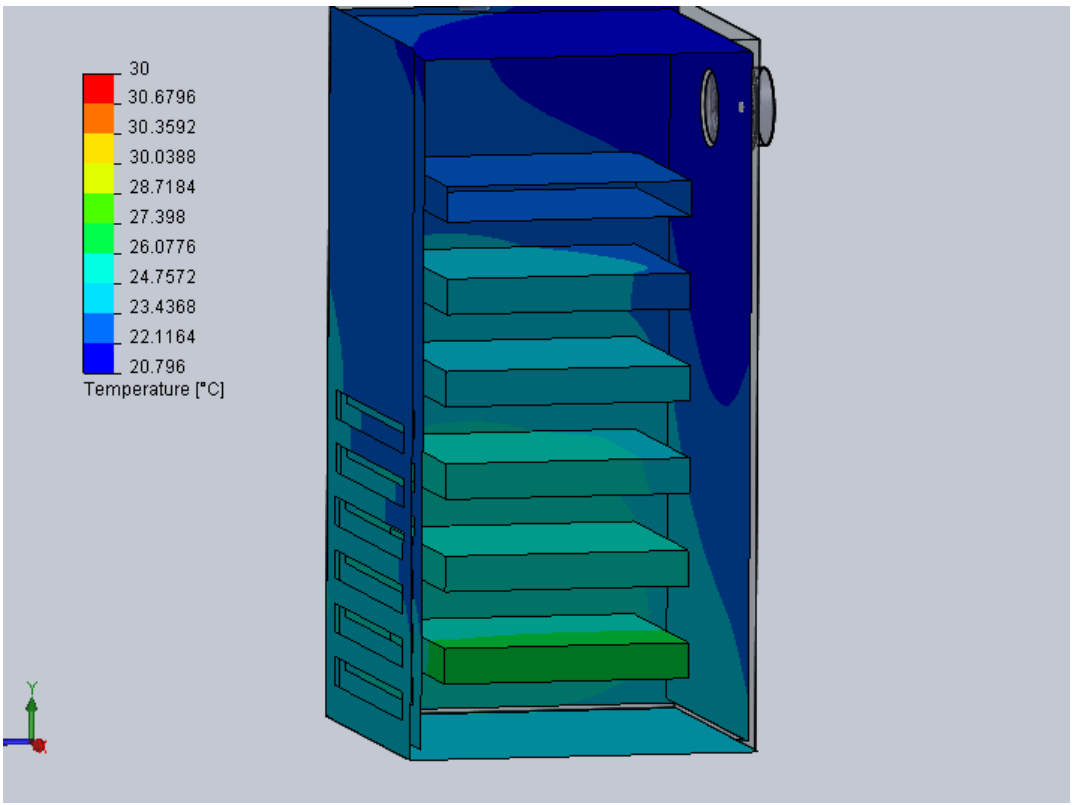

Figure 3.14 : Design-3-temperature distribution of the server with surface plot

3.4 Discussion of Results of the Mechanical Designs.

The air flow rate is shown with cut plot and velocity lines in the previous figures belonging to the all designs show that the airflow is higher in upper part of the server chassis than the lower part, which is expected. Even though the ventilation flow lines do not circulate uniformly, this will not create problem because the air inlet holes are opened at the bottom of the chassis. This makes sure that the air touches every heat-dissipating unit before exiting through the fan. Chassis design and the place where the fan is located are important criteria in ventilation efficiency. However, these criteria are not primary focus in this project.

The first design has nine blades with Ø190 mm. Second design has ten blades with same diameter. Last design has eleven blades with Ø200 mm. Results of the all three designs are summarized in table-3.4. These results state that the best results are obtained by design -1. However, in design-3, more impellers are used with bigger diameter, resulting higher material cost. This causes increase in torque, which leads to bigger size motor. Eventually, this design does not have high efficiency/cost ratio. On the other hand, second design does not provide effective ventilation due to low flow rate even though its torque value is high. The efficiency value is also small compared to the other designs. This is because increasing the number of blades with same diameter causes blade overlapping. The optimum efficiency is obtained as a result of the design-1.

Table 3.4: Comparison of the three designs

	Pressure Head [Pa]	Max Torque [Nm]	Flow Rate [m^3/h]	Efficiency of Fan
Design-1	63	0.37	850	77 %
Desgin-2	100	1.43	870	30 %
Design-3	150	1.5	1100	70 %

3.5 Torque & Speed Characteristic of Fan (Load)

The torque and speed characteristic of the load is very important criteria in the determining the pre-design parameters of the motor. The most important things we need to know about the load are the steady-state torque-speed characteristic, and the effective inertia as seen by the motor. In addition, we clearly need to know what performance is required. At one extreme, for example, in a steel-rolling mill, it may be necessary for the speed to be set at any value over a wide range, and for the mill to react very quickly when a new target speed is demanded. However in fan applications for example, a large ventilating fan, the range of set speed may be quite limited (perhaps from 80% to 100%); it may not be important to hold the set speed very precisely; and the time taken to change speeds, or to run up from rest, are unlikely to be critical.

The torque and speed characteristic of the ventilation fan is determined by both simulation and experiment. Firstly, the designed impeller is analyzed with the help of FEM program in order to derive its torque values at certain speeds. The result of the FEM analysis is given in figure-3.15.

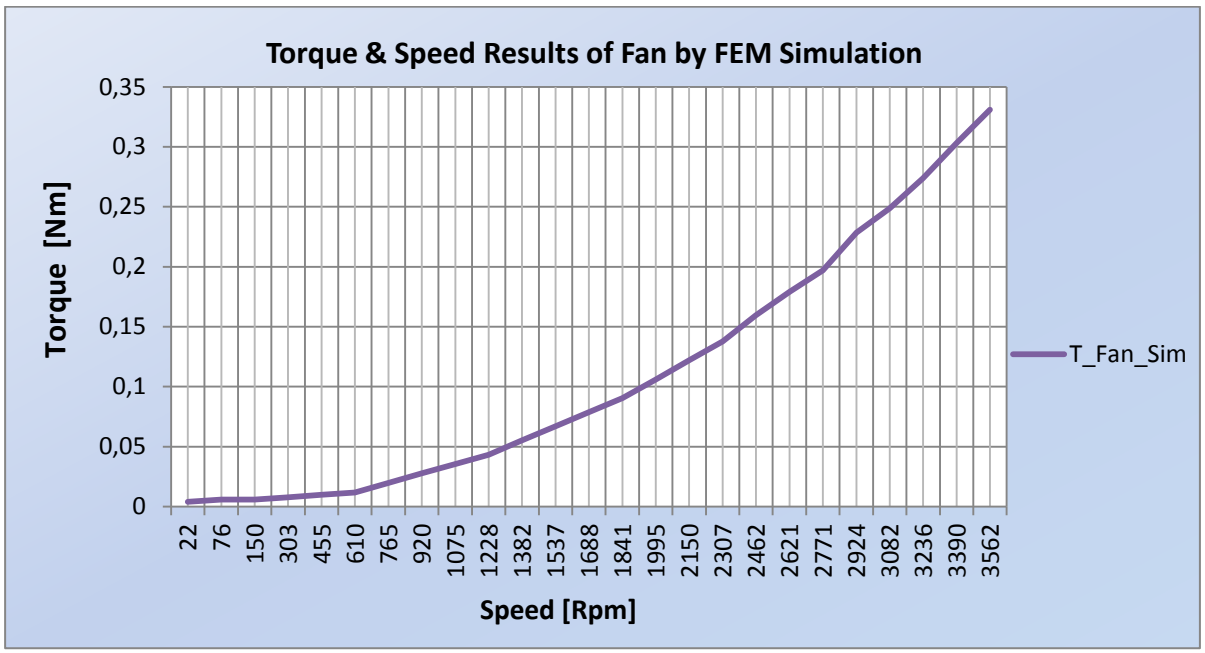

Figure 3.15 : Torque & speed results of fan by FEM simulation

The torque and speed characteristic of fan load is also obtained experimentally. A DC servo motor whose torque constant is known is used in the experiment. A coupling component is prepared in order to connect the fan load to the servo motor. The experiment set-up is shown in figure-3.16. Firstly, the motor is run without any load at some certain speeds ranging from 0 rpm to 3500 rpm. All current and speed values are recorded. Then, the motor is loaded with fan and all current values are recorded under the same certain speeds. Then according the torque formula as given in equation-3.1, torque values of the fan load are calculated.

$$T_{FAN} = K_T(I_L - I_o) \qquad \textbf{(3.1)}$$

where the K_T is torque constant, I_L and I_O are the currents with and without load respectively.

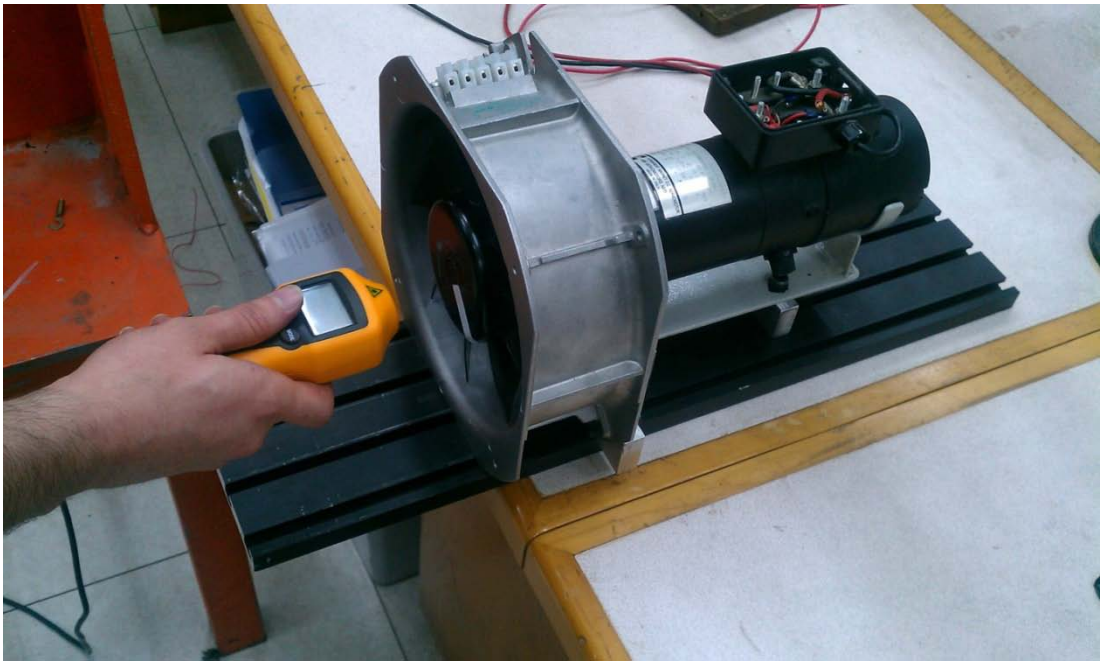

Figure 3.16 : Fan load experiment set-up

As a result of this calculation, the torque and speed characteristic is given in figure-3.17. T_L and T_O are the torque values with and without load respectively as shown in figure-3.19. Figure-3.18 also shows that comparison of results of FEM simulation and experiment. Very small difference is observed, which is expected because of the difference between experimental setup and simulation environment.

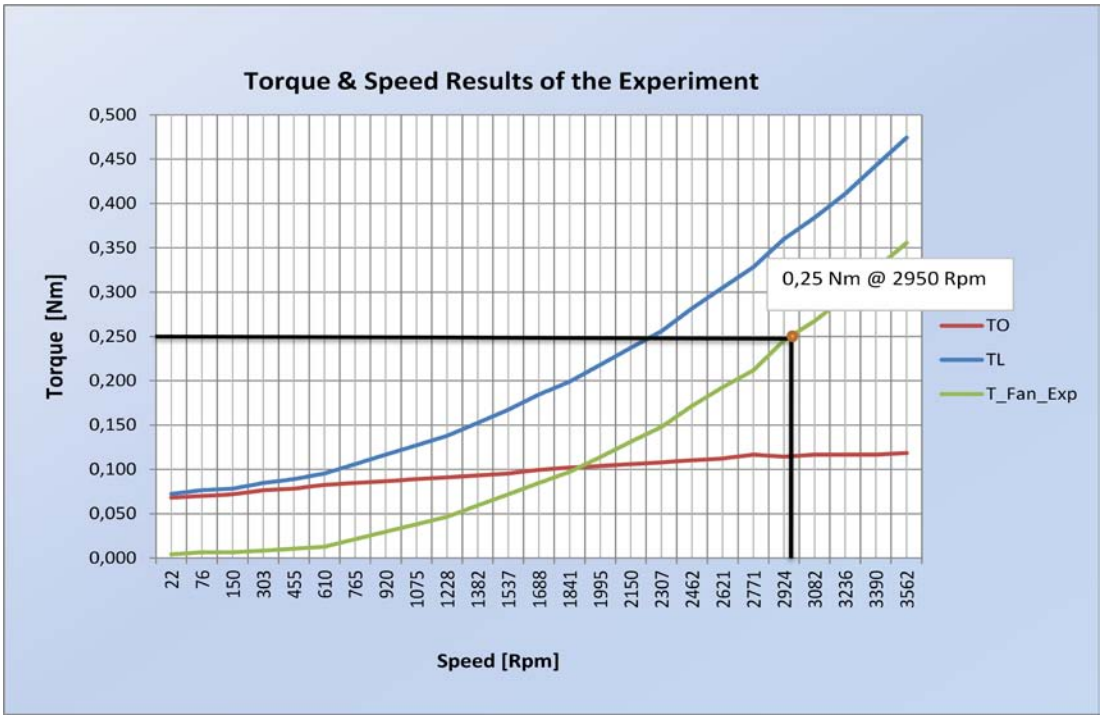

Figure 3.17 : Torque and speed characteristics of the fan derived experimentally

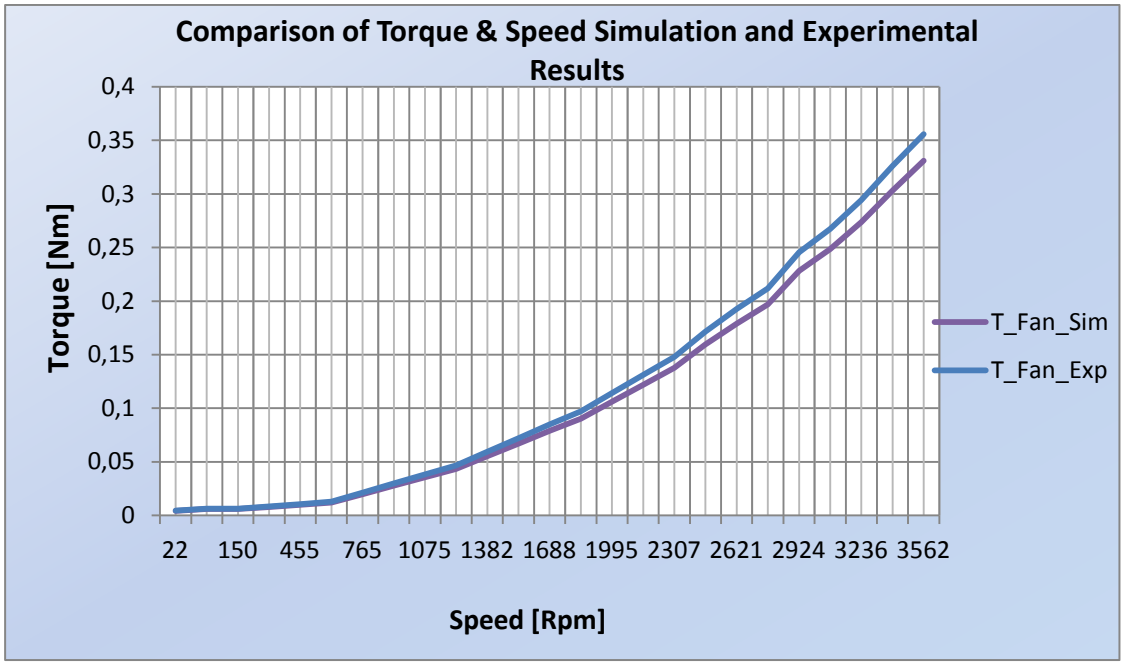

Figure 3.18 : Comparison of torque and speed results of the simulation and experiment

3.6 Design Parameters for the Single Phase PMBLDC Motor Fan

The design parameters are determined according to the both experimental and simulation results. Design parameters of the fan are determined according to the flow simulation results obtained in design-1. Motor specifications are determined according to the environment in which this fan motor is going to be used. All design parameters are as shown in table-3.5.

Table 3.5: Design parameter of the single phase PMBLDC motor fan

FAN SPECIFICATIONS	Impeller Diameter	[mm]	Ø190
	Blade Numbers	[#]	9
	Housing Diameter	[mm]	Ø200
	Flow Rate	[m^3/h]	850
	Max. Torque	[Nm]	0.37
	Average Torque	[Nm]	0.25
	Pressure Increase	[Pa]	63
	Efficiency	[%]	77
MOTOR SPECIFICATIONS	Motor Type		Single Phase PMBLDC
	Supply Voltage	[Volt]	24
	Nominal Current	[A]	2-2.6
	Input Power	[Watt]	50-60
	Speed	[Rpm]	2950-3000

4. MAGNETIC ANALYSIS and DESIGN of SINGLE PHASE PMBLDC MOTOR

4.1 Physical Dimensions of the Single Phase PMBLDC Motor

Single-phase PMBLDC motor is going to be designed as outer rotor structure in order to get better efficiency in ventilation application. Outer rotor structure provides two important advantages. First advantage is that flowing of the air through the blades by touching the outer part of the rotor will reduce the motor working temperature. Another advantage is that the outer rotor structure protects the inside of the motor against oils, dusts and different external particles. Furthermore, six-pole stator and six-pole rotor construction are chosen in order to increase torque performance (Figure-4.1). The initial physical dimensions are given in table-4.1.

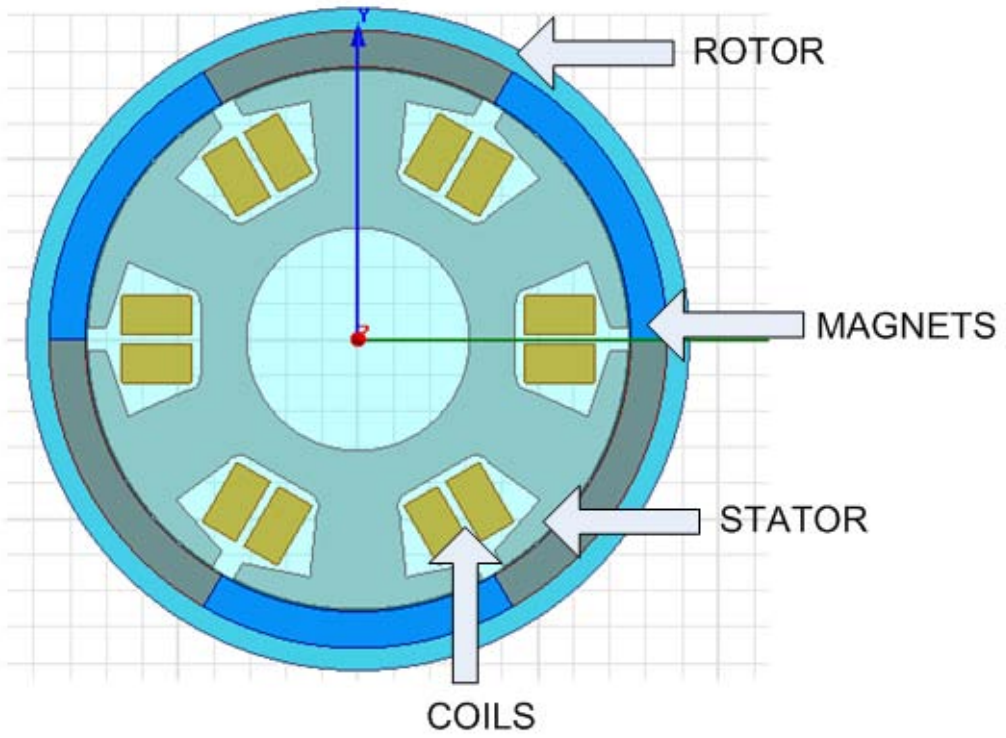

Figure 4.1: Single phase PMBLDC motor structure

Table 4.1: Initial dimensions of PMBLDC motor

Rotor	Outer Diameter	92 mm
	Inner Diameter	75 mm
Stator	Outer Diameter	75 mm
	Inner Diameter	31 mm
Magnets	Outer Diameter	75 mm
	Inner Diameter	65 mm

4.2 Magnetic Design of the Single Phase PMBLDC Motor

The magnetic design is started with symmetric air gap and continues with asymmetric air gap approximations. In all designs, 6x6 external motor structures are used with different dimensions.

4.2.1 Design-1: symmetric air gap:

In this design, 6x6 PMBLDC motor is simulated by FEM techniques. The initial dimensions given in table-4.1 are used in this design. The magnet embrace is taken as 1. The air gap is 0.5 mm. Four switching components are used in order to provide rotating magnetic field. The input current is not limited in order to see the transient current. The results are shown in figure-4.2. First graph of the figure-4.2 shows the moving torque of the motor. The average torque is 0.005 Nm while the maximum torque is 0.6 Nm. The torque values are very low due to the fluctuations. These fluctuations are expected since air gap is uniform. Second graph indicates the current drawn by the coil. As it is observed, it is positive in one cycle and negative in second cycle. The full cycle is 120^0 in electrical angle. We observe the flux linkages of the coil in the third graph. It is the flux linkage of 47 turns in one tooth. The value of the flux linkage reaches to 26 mWb. Fourth graph shows the back-emf of the coil. The spikes are observed at the switching time.

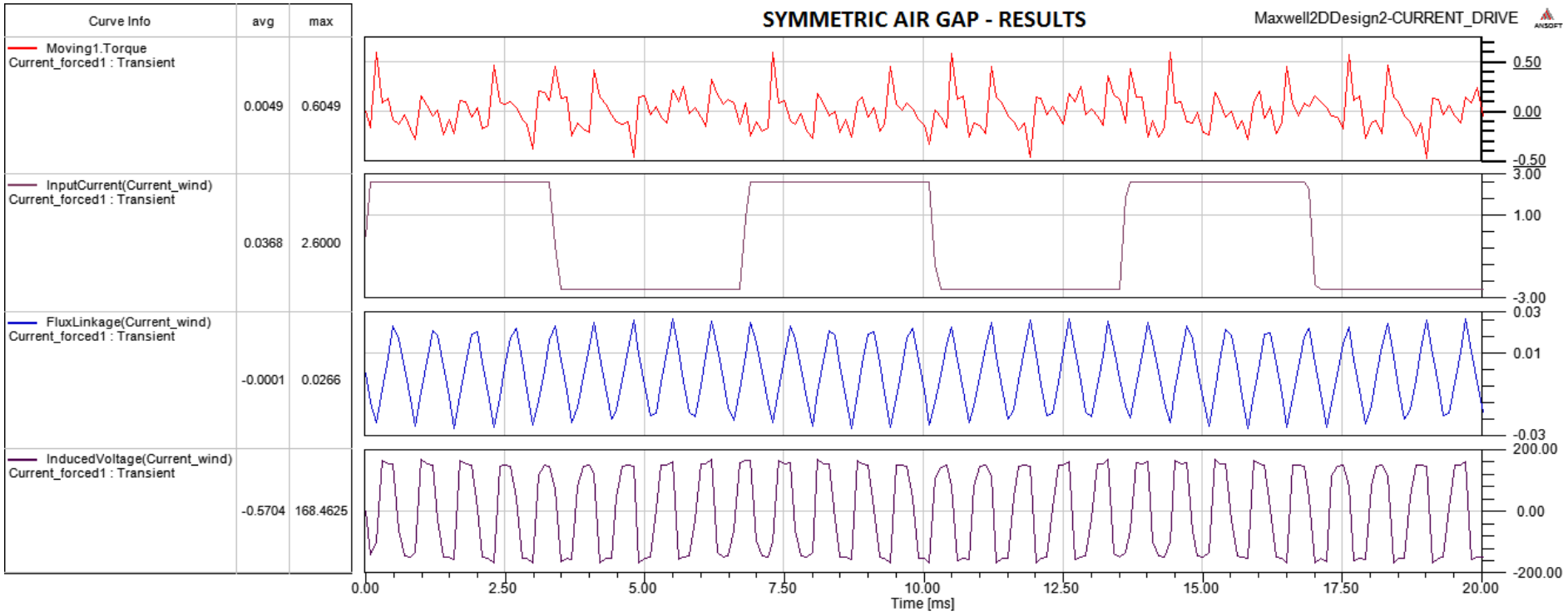

Figure 4.2: General results of the symmetric air gap design

Magnitude of the magnetic field vector is shown in figure-4.3 and figure 4.4. The scale is ranging from 7 mTesla to 3.3 Tesla. The magnetic field is distributed uniformly and it shows that the materials, such as rotor, stator and magnet, do not saturate while motor is rotating. Magnetic field is close to saturation only in the points where the ends of the magnets are touching each other. This is expected since the magnetic flux lines of the two neighboring magnet are combining and creates much more magnetic field at that location.

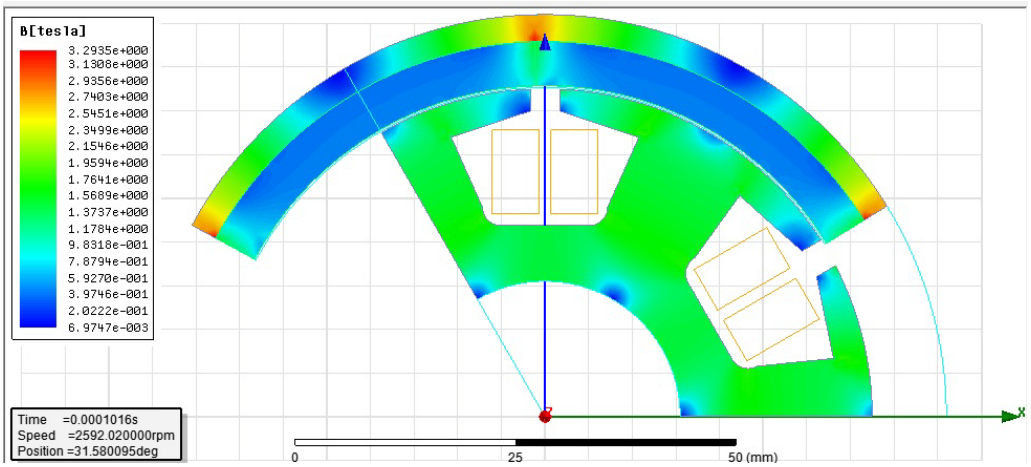

Figure 4.3: Design-1-magnetic field distribution of symmetric air gap model

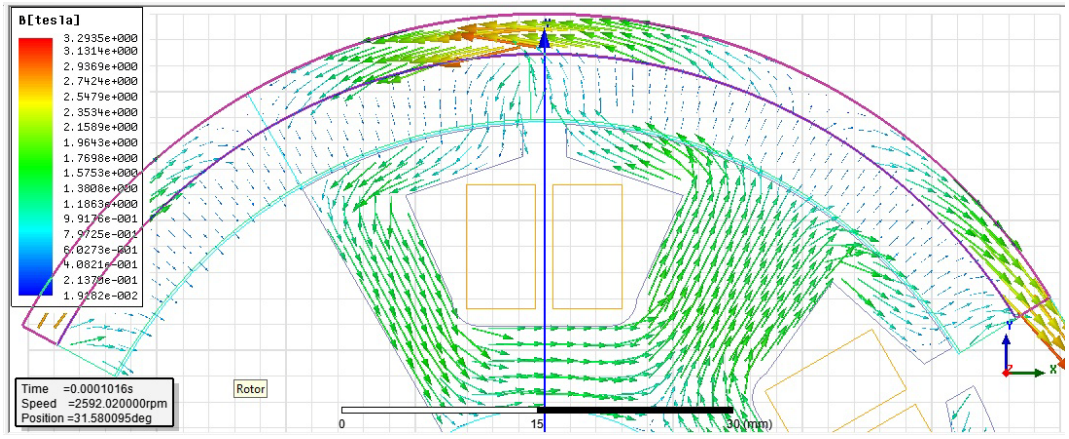

Figure 4.4: Design-1-magnetic field vector of the of symmetric air gap model

4.2.2 Design-2: asymmetric large air gap model

Uni-directional rotation will be obtained by using asymmetrical air gap between stator and rotor magnet as shown in figure-4.5. The aim of this structure is to obtain a uni-directional movement with low start-up current while maintaining required torque. In this design, air gap size is changed in such a way that maximum air gap size is 1.84 mm and minimum air gap size is 0.35 mm. The difference between maximum and minimum air gap is about 1.5 mm (Figure-4.5).

Mesh operation is very critical step in FEM analysis in order to get correct results. Since the air gap has asymmetry, special dense meshes are assigned between rotor and stator. The mesh plot of the PMBLDC motor is shown in figure-4.6.

The results of the "Large Air Gap" model are given in figure-4.7. The first graph of the figure-4.7 shows the torque output of the motor. The average value of the torque is 0.42 Nm despite of the fluctuations. The maximum value is obtained as a result of the FEM simulation is 0.61 Nm. These fluctuations are expected since the motor has single-phase winding arrangement. The current waveform is observed in the second graph. The nominal current is 2.6 A. The third graph indicates the flux linkages of the winding on the stator. The value changes from -78.5 mWb to 78.5 mmWb. The last graph shows the back-EMF induced in the coils, which is created due to the rotation of the magnets. The value of the back-Emfs is changing from -61 Volt to 57 Volt.

Magnitude of the magnetic field vector is shown in figure-4.8 – 4.15. The scale is ranging from 1.3 mTesla to 2 Tesla. The stator, rotor and magnets do not saturate and the working point is in the linear area of the BH curve. The stator experiences maximum magnetic field while the rotor is aligning with the stator teeth. This situation is observed when the rotor is 0^0 in electrical degree as shown in figure-4.8. Magnetic field increases considerably on the teeth of the stator as shown in figure-4.15. This is because the field lines of the two neighboring magnets are coming together at that position and causes the stator teeth to approach 2 Tesla.

Magnetic field in the rotor is close to saturation only in the points where the ends of the magnets are touching each other. This is expected since the magnetic flux lines of the two neighboring magnet are combining and creates much more magnetic field at

that location. In the third design some improvements will made in order to reduce density of the magnetic field at these locations.

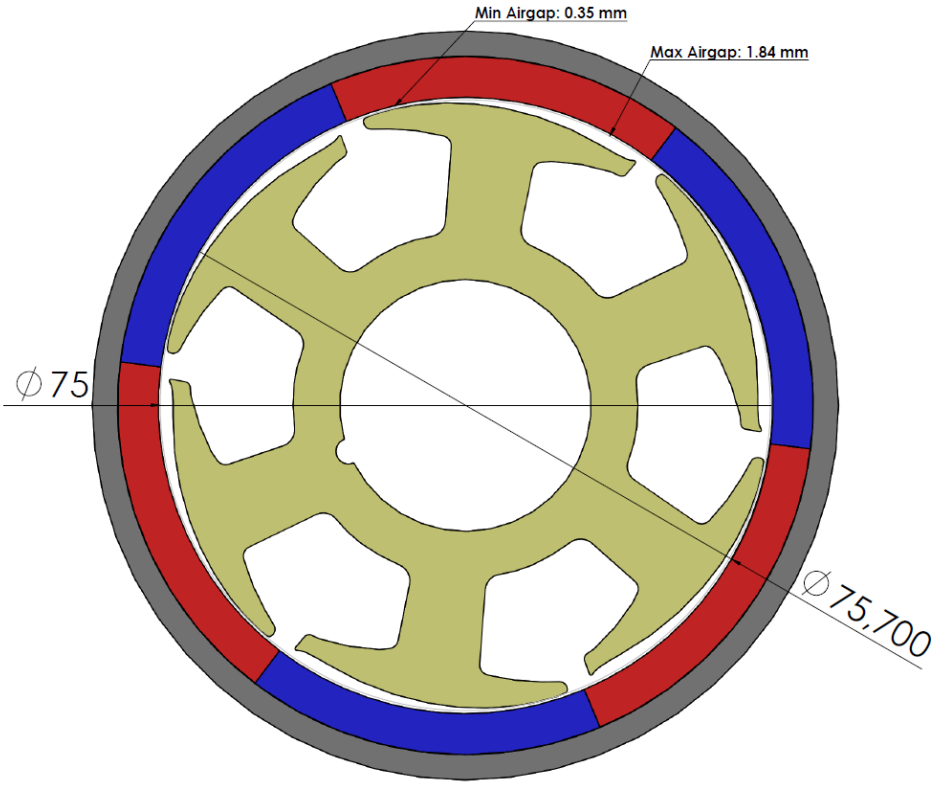

Figure 4.5: "Asymmetric large air gap" motor structure

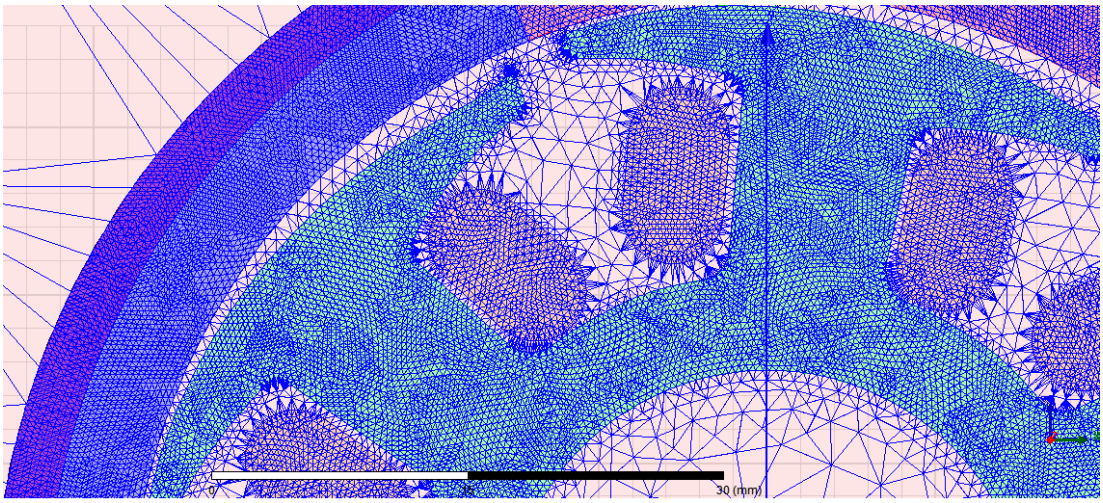

Figure 4.6: Mesh plot of the "asymmetric large air gap" motor model

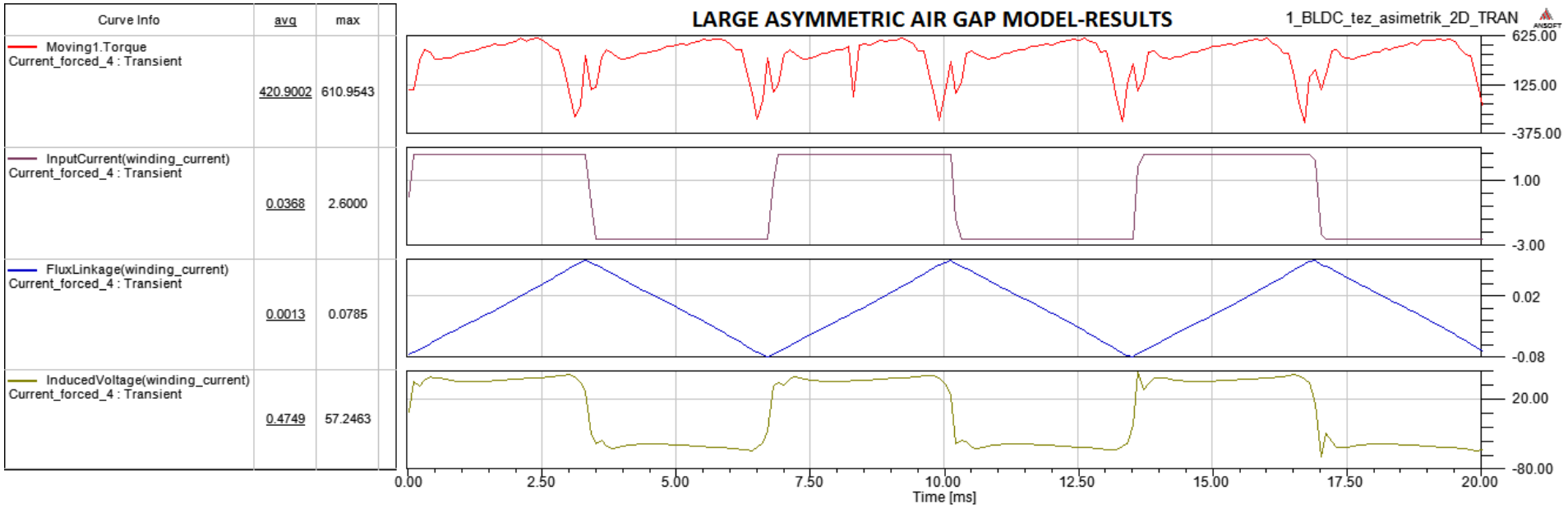

Figure 4.7: Results of the “asymmetric large air gap model”

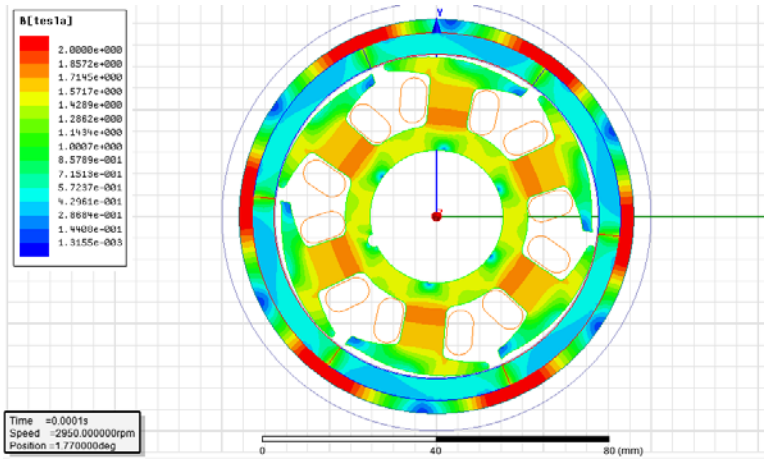

Figure 4.8: Magnetic field distribution of asymmetric large air gap model (electrical position : 0^0)

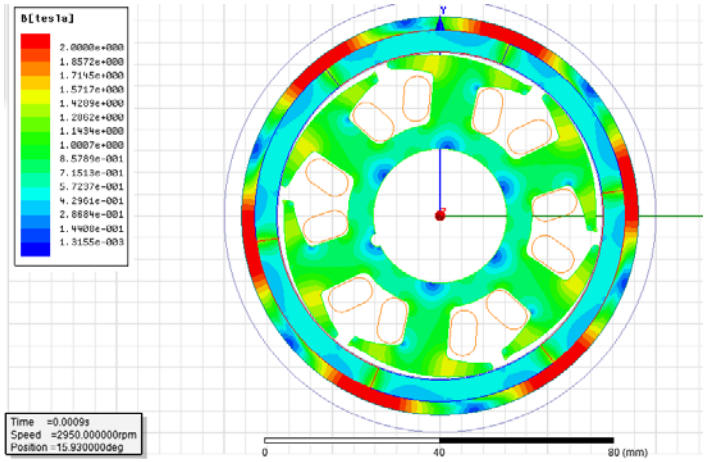

Figure 4.9: Magnetic field distribution of asymmetric large air gap model (electrical position : 15^0)

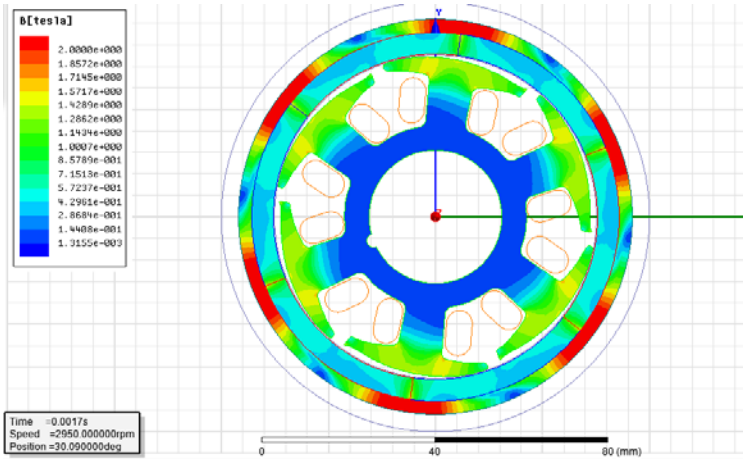

Figure 4.10: Magnetic field distribution of asymmetric large air gap model (electrical position : 30^0)

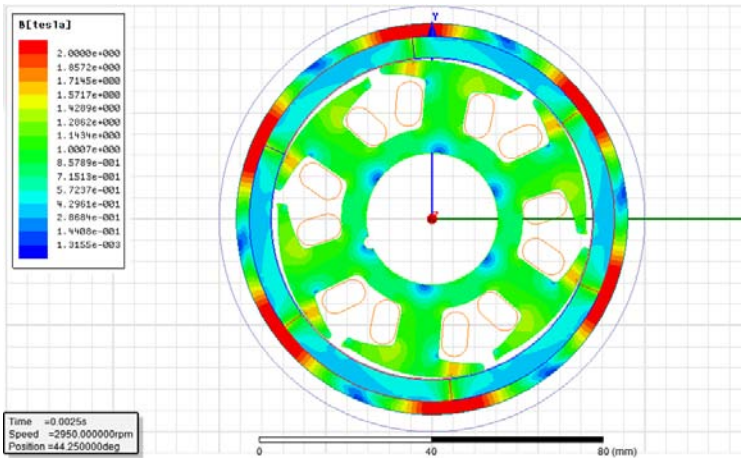

Figure 4.11: Magnetic field distribution of asymmetric large air gap model (electrical position : 45^0)

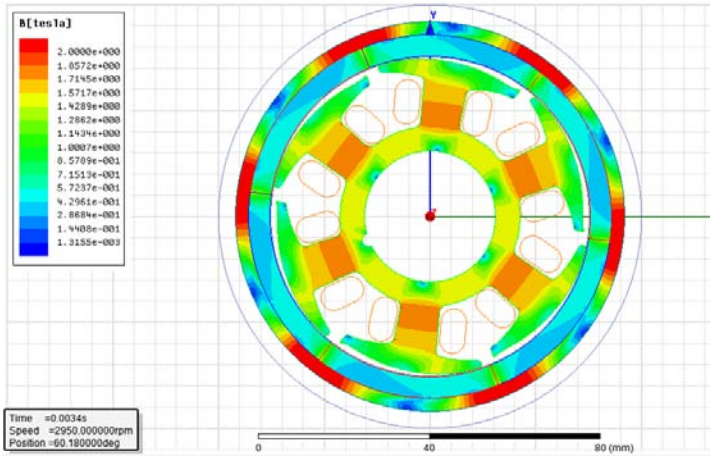

Figure 4.12: Magnetic field distribution of asymmetric large air gap model (electrical position : 60^0)

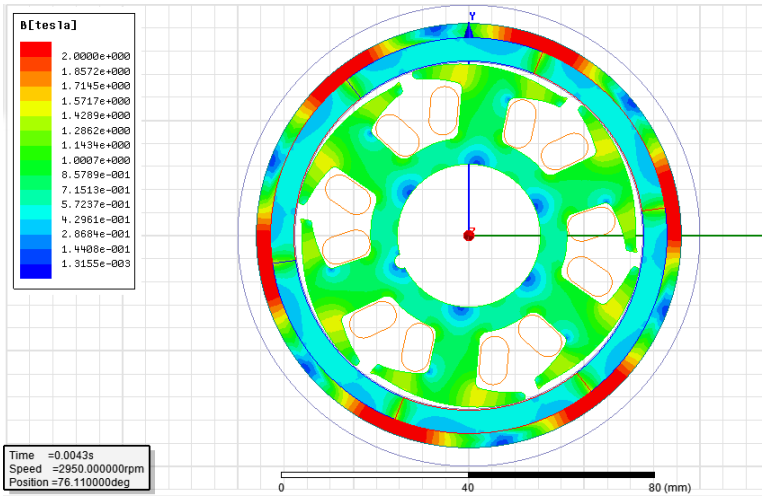

Figure 4.13: Magnetic field distribution of asymmetric large air gap model (electrical position : 75^0)

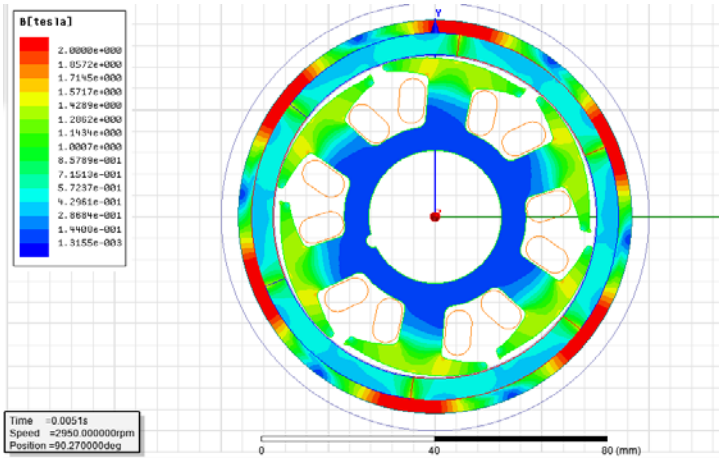

Figure 4.14: Magnetic field distribution of asymmetric large air gap model (electrical position : 90^0)

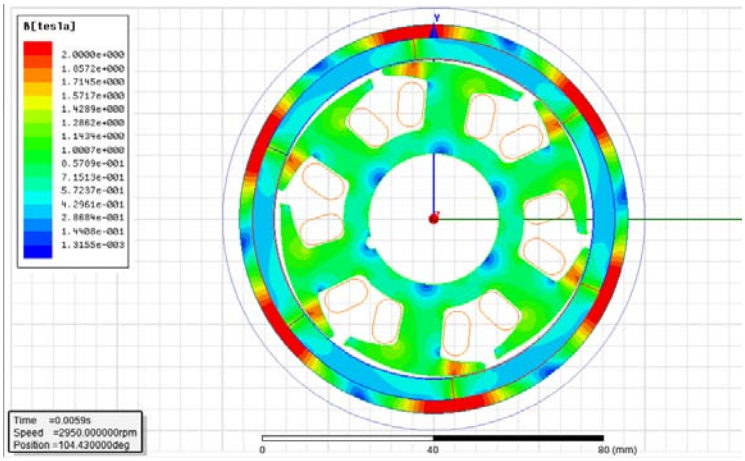

Figure 4.15: Magnetic field distribution of asymmetric large air gap model (electrical position : 105^0)

4.2.3 Design-3 : asymmetric small air gap model

In this design, air gap size is changed so that maximum air gap becomes 1.2 mm and minimum air gap is 0.6 mm (Figure-4.16). The difference between maximum and minimum air gap becomes 0.6 mm. Besides, it is observed that the magnetic field lines create magnetic field density in tooth region of the stator in the design-2. Therefore, the neck thickness of the teeth is increase by 2 mm from both sides. The teeth thickness is also increased by about 0.5mm-1mm. The mesh plot of the small air gap PMBLDC motor is shown in figure-4.17.

The general results of the asymmetric small air gap design are given in figure-4.18. First graph of the figure-4.18 shows the output torque. The motor has average torque 0.42 Nm and maximum torque is 0.55 Nm.. The minimum torque values is generated 0 Nm at position 40^0. The fluctuations observed are reduced considerably due to the improvement achieved in air gap design. The current waveform is observed in the second graph. The nominal current is 2.6 A. The third graph indicates the flux linkages of the stranded conductor in each tooth. The flux linkages values change from -82 mWb to 82 mWb. Last graph shows the induced back-emfs. The value of the generated back-emfs is 81 V.

Magnetic field lines are distributed as shown in from figure-4.19 to figure-4.26. The scale is ranging from 0.1 mTesla to 2 Tesla. The rotor, stator and magnets do not reach the saturation while motor is working at nominal speed. For the rotor, the critical region is the points where the ends of the two magnets are touching. However, it is not possible to increase the rotor diameter, which will reduce the impeller surface area, as a result reduction is created in the flow rate which is not desired in overall design.

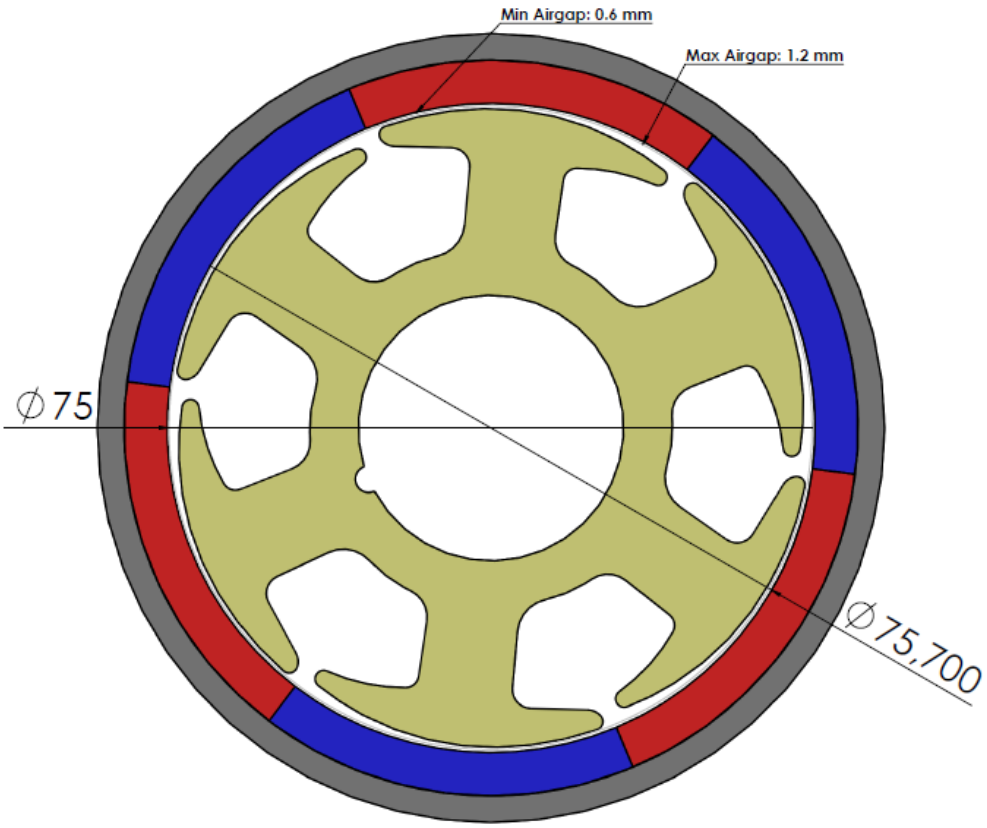

Figure 4.16: "Asymmetric small air gap" motor structure

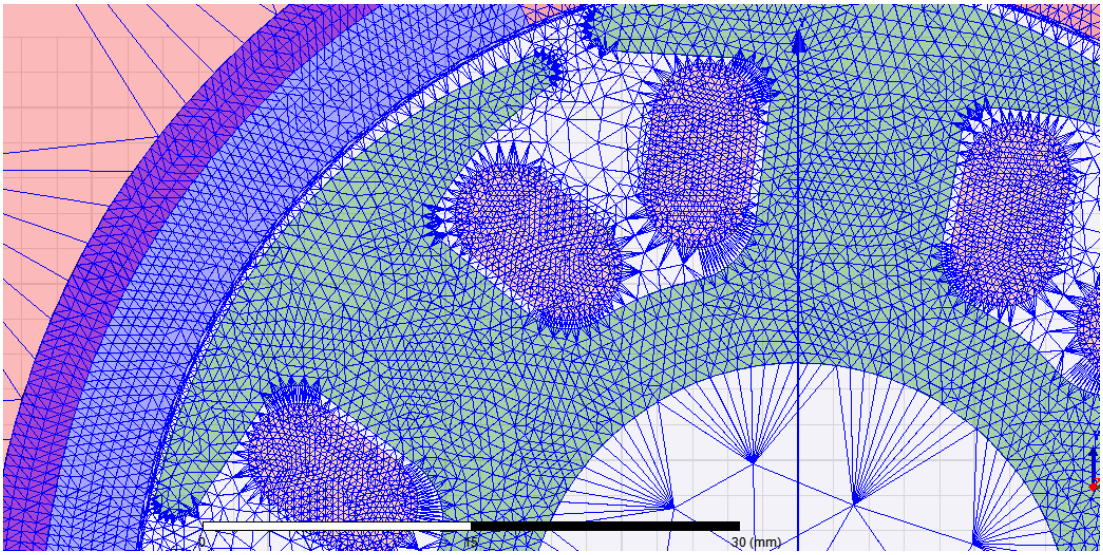

Figure 4.17: Mesh plot of the "asymmetric large air gap" motor model

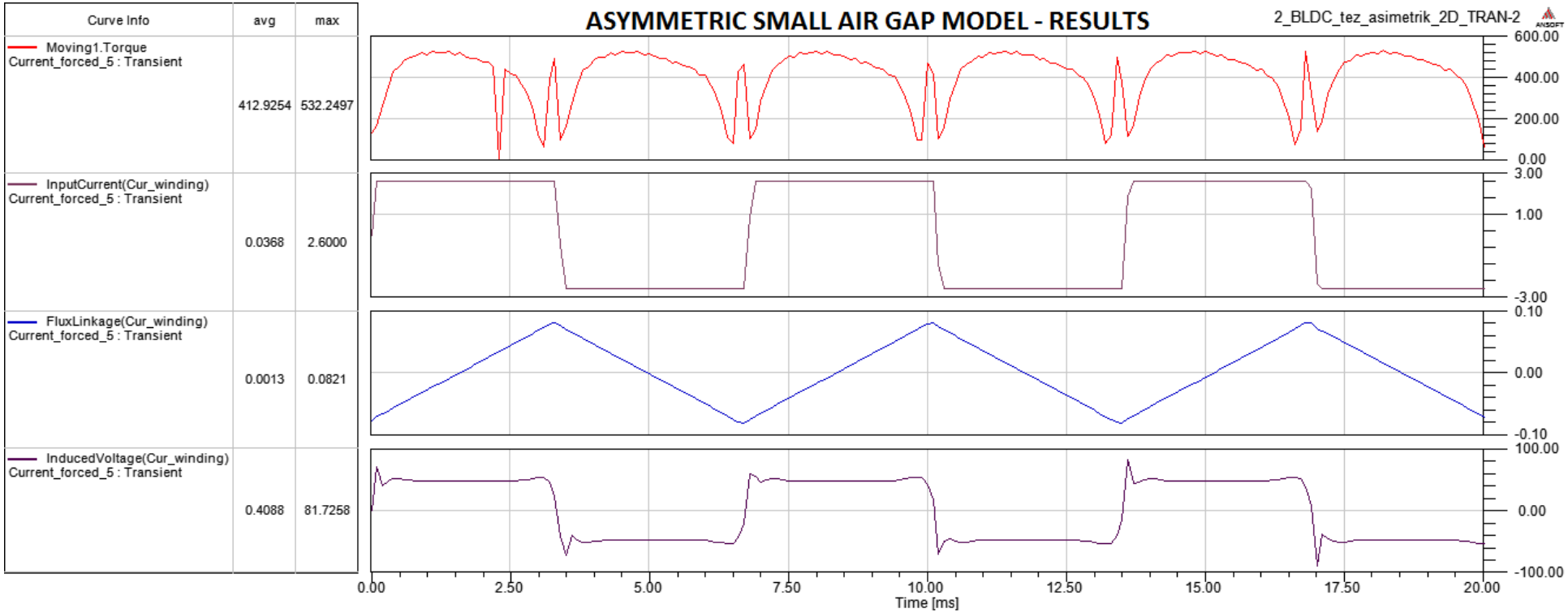

Figure 4.18: Results of the “asymmetric small air gap model

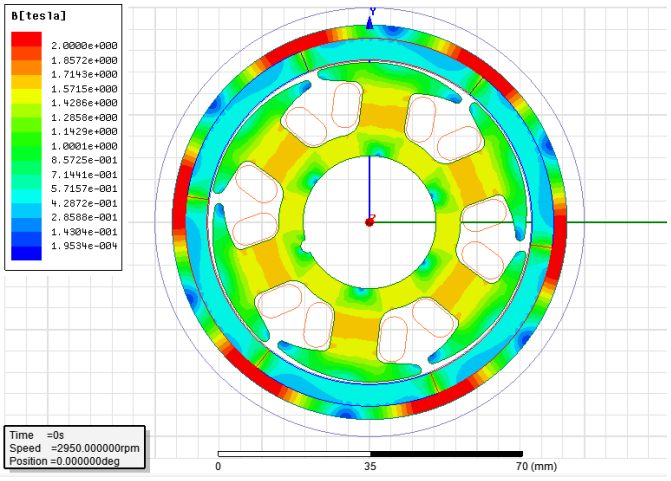

Figure 4.19: Magnetic field distribution of asymmetric small air gap model (electrical position : 0^0)

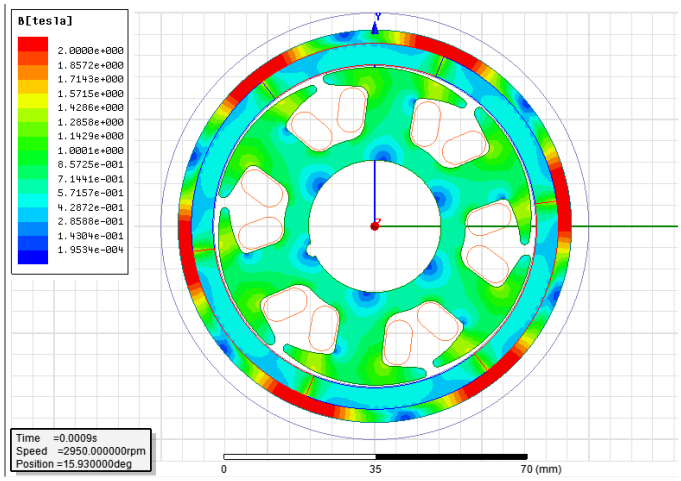

Figure 4.20: Magnetic field distribution of asymmetric small air gap model (electrical position : 15^0)

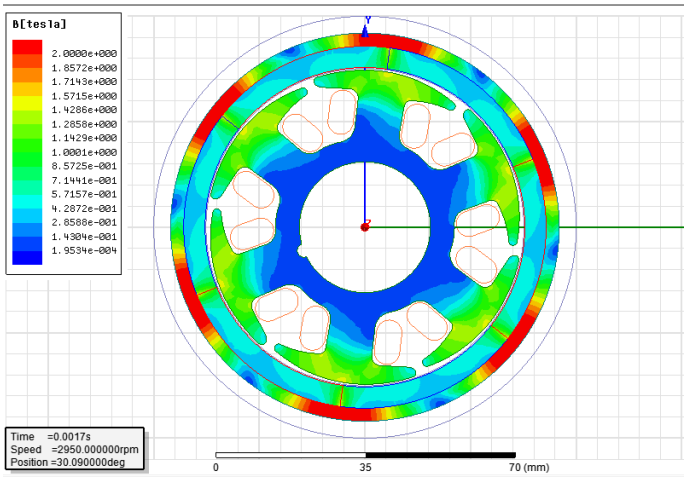

Figure 4.21: Magnetic field distribution of asymmetric small air gap model (electrical position : 30^0)

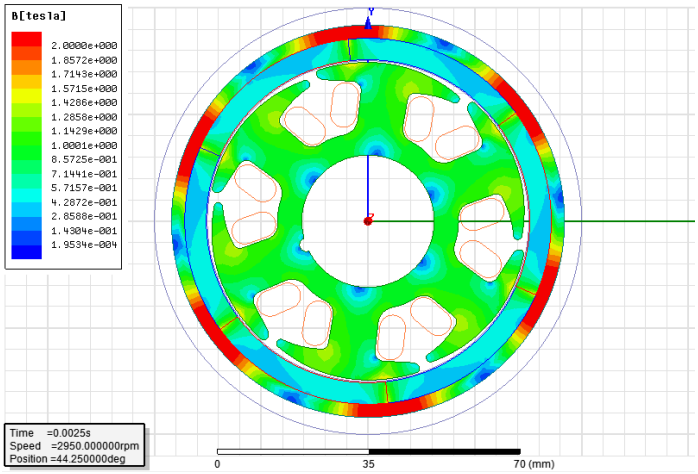

Figure 4.22: Magnetic field distribution of asymmetric small air gap model (electrical position : 45^0)

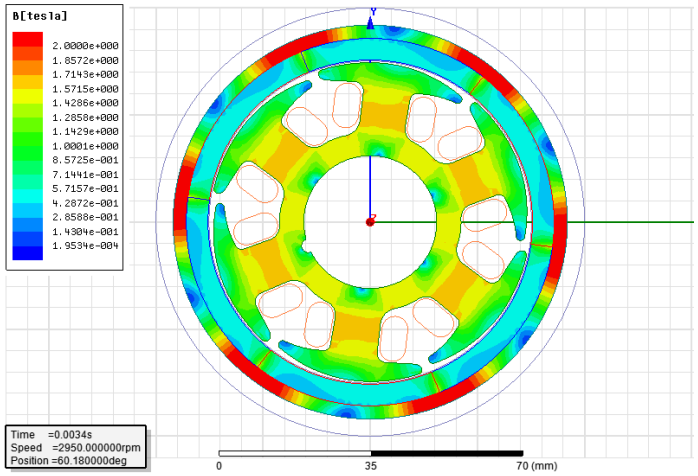

Figure 4.23: Magnetic field distribution of asymmetric small air gap model (electrical position : 60^0)

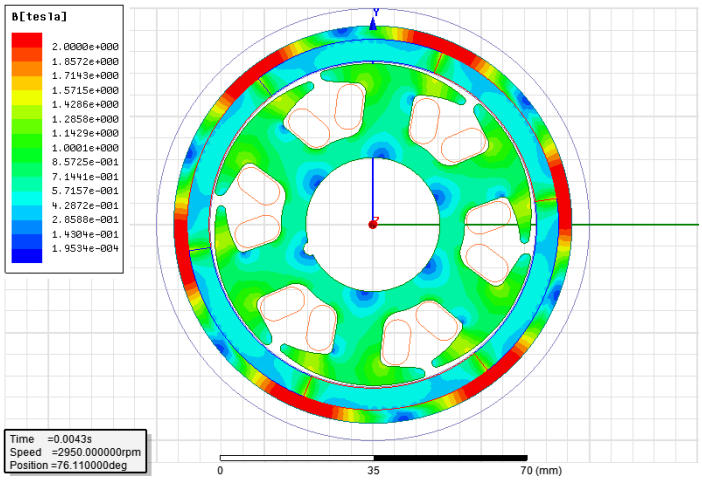

Figure 4.24: Magnetic field distribution of asymmetric small air gap model (electrical position : 75^0)

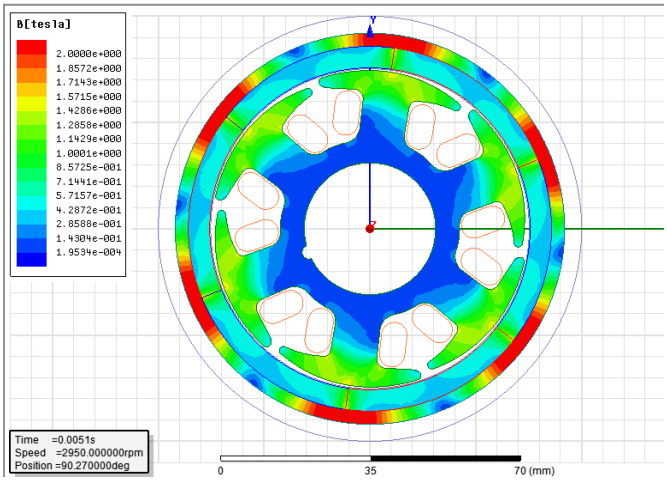

Figure 4.25: Magnetic field distribution of asymmetric small air gap model (electrical position : 90^0)

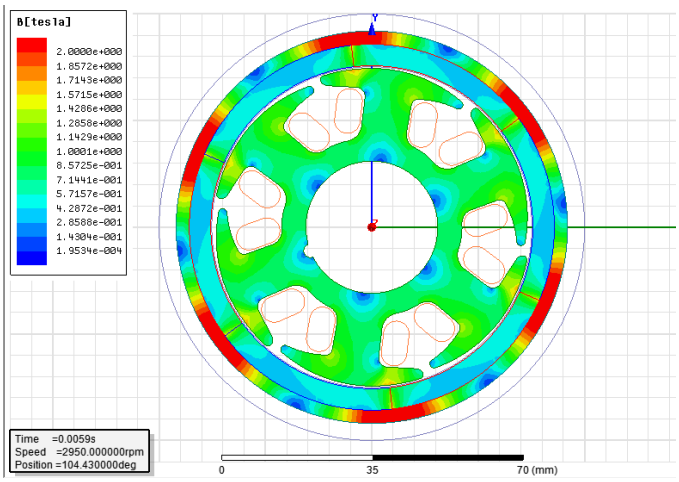

Figure 4.26: Magnetic field distribution of asymmetric small air gap model (electrical position : 105^0)

4.2.4 Influence of the switching angle on the PMBLDC motor performance

Another important point in the design of the PMBLDC motor is to determine the angle at which the switching should be done. Due to the high-speed operation, the winding inductance causes a significant phase delay in the current waveform. The results in the current and the emf waveforms being out of phase, and a negative torque component is generated, with a consequent reduction of the overall torque. Phase commutation advanced is often employed in order to achieve better motor performance. In DC brush motor the commutation angle is determined by the position of brushes and is kept constant. In BLDC motors the switching angle may vary accordingly to the controller of the inverter that is used [14].

The position sensor is placed somewhere in between 0^0 - 120^0 electrical angle in single phase PMBLDC motor. This sensor senses the position of the rotor and triggers the transistors so that they switch on the correct polarity of the winding.

As the switching angle is advanced, the difference between back-emf and the supply voltage increases, and the torque thereby increases. However, there exists an optimal advanced angle, beyond which the drive performance deteriorates. The simulation was done for the following switching angles 0^0, 15^0, 30^0, 45^0, 60^0. Figure-4.27 shows that the sensor should be placed in 0^0 degree to get maximum average torque. The 0^0 electrical angle is the position at which the magnets of the rotor are aligned with the teeth of the stator.

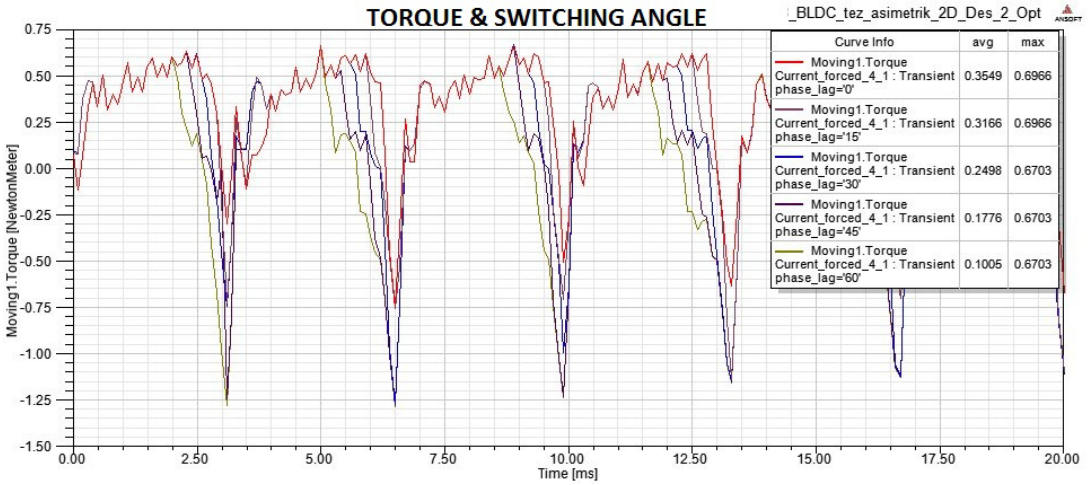

Figure 4.27: Output torque for the different switching angles.

4.3 Discussions of the Results

Three different designs are analyzed by using FEM techniques in terms of magnetic perspective. 6x6 PMBLDC motor with symmetric air gap is simulated in the first design. In the second design, the air gap is changed and the asymmetric air gap model is generated. This asymmetric model is simulated under special mesh assign. In the last design, improvement is achieved over the second design by changing the air gap model so that difference between maximum and minimum air gap size becomes 1.5mm. The simulation of the last design is also achieved successfully.

Table 4.2: Result of the all magnetic analysis and designs

		Design-1: Symmetric Air Gap	Design-2: Asymmetric Large Air Gap	Design-3: Asymmetric Small Air Gap
Torque [Nm]	Max.	0.6	0.61	0.55
	Avg.	0.005	0.40	0.42
	Min.	-0.48	-0.25	0.1
Nominal Current [A]	Max.	2.6	2.6	2.6
	Avg.	-	-	-
	Min.	-2.6	-2.6	-2.6
Flux Linkage [mWb]	Max.	26	78.6	82
	Avg.	0.1	1.3	1.3
	Min.	-26	-78.5	-82
Back EMF [Volt]	Max.	168	57	81
	Avg.	-0.5	0.5	0.4
	Min.	167	-61	-88

The results of each design are given in table-4.2. It is easily can be observed that the symmetric air gap model is not efficient due to the generating low average torque. The back emfs is also very high, that causes reduction in torque. In the second design, asymmetric air gap model is achieved with some successes. Even though an effective average torque is generated, the fluctuations are very high. This will cause the motor generating high noise and vibrations. The difference between maximum and minimum torque is 0.86 Nm. This torque difference is going to be reduced in the last design. In the last design, asymmetric air gap model is improved so that the torque fluctuations are reduced considerably. Even though the driving current waveforms are same for both design-2 and design-3, the torque fluctuations are reduced because of the improvement achieved in the air gap model. In design -3, the star-up current is also reduced due to the low air gap resistance.

Another important point is the switching angle. The performance of the motor may dramatically change when the switching angle is changing. Figure-4.27 shows the torque results of the motor with different switching angles. It becomes obvious that the best efficiency is obtained by placing sensor in between two-stator tooth. This is also shown in figure-4.28.

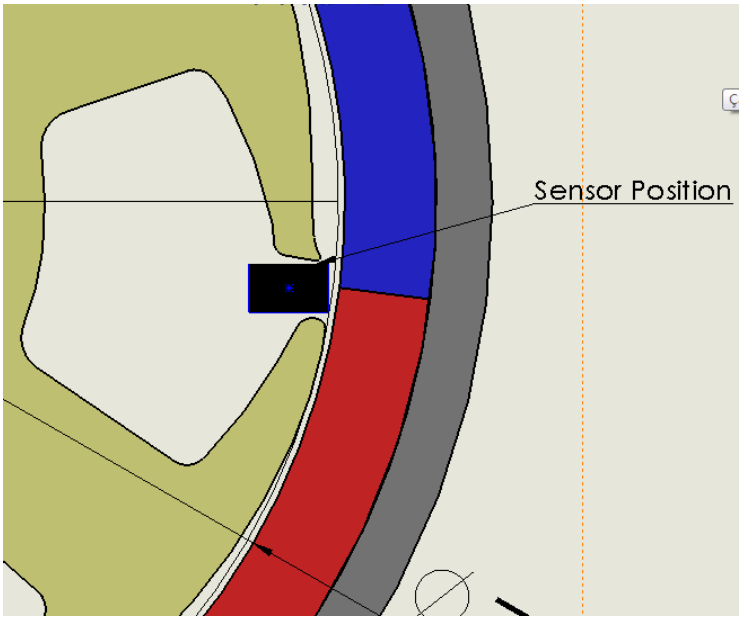

Figure 4.28: Sensor position in the motor

Lastly, the results of the magnetic analysis are compared with results of the mechanical analysis. In the mechanical analysis phase, impeller with nine blades, whose diameter is 190mm is chosen as an optimum load. The motor designed in the magnetic analysis phase must have enough output characteristic in order to fulfill the requirements needed by load. The results are shown in table-4.3. The motor output torque is high enough to rotate the required fan load. The motor rotates at 2950 min^{-1} that is very similar to the nominal fan speed.

Table 4.3: Comparison of the results of the mechanical and magnetic designs

	FAN SPECIFICATIONS	MOTOR SPECIFICATIONS
Max. Torque	0.37 Nm	< 0.55 Nm
Average Torque	0.25 Nm	< 0.42 Nm
Speed	2950 min^{-1}	= 2900 min^{-1}

5. CONCLUSION

Design and the implementation of single-phase PMBLDC motor for low power fan applications are investigated under the scope of the project. The design stage is divided into two steps: first step is the design of mechanical parts such as impeller and housing under real environmental conditions, second step is design of the PMBLDC motor by focusing on the magnetic analysis.

Mechanical parts of the fan are designed by considering the efficiency of the fan in the environmental conditions, which are simulated by FEM method. The fan is simulated with the designed impeller and housing and the result are discussed in terms of efficiency. The velocity profiles of the fan and temperature distribution are given in details to verify the correctness of the mechanical designs. Then the torque and speed curve is derived as a result of the FEM simulation. The result of the simulation is verified by the results of experiment set-up. After these steps, the design parameters that are required for designing single phase PMBLDC motor are determined. These parameters are velocity of the motor, supply voltage and torque & speed characteristic of the motor.

In the second phase of the project, the magnetic design and analysis have been achieved. Three different design approximations are simulated and effective results are obtained. These results are compared and small asymmetric air gap structure is chosen as an optimum design due to the less torque fluctuations and lower start-up current. The only limitation is that asymmetric motor structure causes motor to rotate in only one direction. However, it is not an important drawback since this motor is used in ventilation applications.

For future work, the drive circuit should be designed and implemented in order to prepare a real motor. The software of the driving circuit should be written according to asymmetric air gap model, which is capable of rotating only in one direction. The cogging torque analysis must be done in order to observe what drawback occur at very low speed.

REFERENCES

[1] **URL** <http://www.ebmpapst.us/techarticles.asp>, accessed at 01.05.2011

[2] **Yılmaz, M.,** 2005. The Application of Wavelet Technique to Sensorless Control of Brushless Direct Current Motor, Istanbul Technical University, November 2005.

[3] **S. Bentouati, Z., Q. Zhu, D. Howe,** 1999. Permanent Magnet Brushless DC Motors for Consumer Products, IEEE Ninth International Conference on Electrical Machines and Drives, No. 468, 1999.

[4] **Bhim Singh, Sanjeev Singh,** 2009. State of Art on Permanent Magnet Brushless DC Motor Drives, Journal of Power Electronics, Vol. 9, No. 1, January 2009.

[5] **Ahmed, S., Lefley, P.,** 2005. Development of a Single Phase PM BLDC Motor from a Novel Generic Model, Technical Paper, Department of Electrical Engineering of University of Leicester, May 2005.

[6] **Jang, G. H., Wasynczuk, O.,** 1989. Analysis and Modeling of Single Phase Brushless DC Motor Drive System, IEEE Transaction on Energy Conversion, Vol. 4, No. 3, September 1989.

[7] **Mayer, J.S., Yeom, J. H., Kim, M. G.,** 2006. Determination of torque–speed–current characteristics of a brushless DC motor by utilizing back-EMF of non-energized phase, MMM - Magnetism and Magnetic Materials 310, 2790-2792, November 2006.

[8] **Kenjo, T., Nagamori, S.,** 1985. Permanent-Magnet and Brushless DC Motor, Oxford University Press, New York

[9] **Bilal Akin, Manish Bhardwaj**, Trapezoidal Control of BLDC Motors Using Hall Effect Sensors, C2000 Systems and Applications Team, Version 1.0, February 2010

[10] **Hanselman, D.C.,** 2003. Brushless Permanent Magnet Motor Design, Mc. Graw Hill Press

[11] **Microchip Technology Inc.**, 2003, Brushless DC (BLDC) Motor Fundamentals, AN885, Application Note, January 2003.

[12] **Honeywell International Inc**., 2009, Hall Effect Sensing and Application, Micro Switch Sensing and Control, Reference Book, April 2009.

[13] **Atmel Corp.,** 2006. Sensor-based control of three phase Brushless DC motor, Application Note, 2596B-AVR-02/06, February 2006

[14] **Nekaubin, Abdolamir** 2011. Design of a Single Phase BLDC Motor and Finite Element Analysis of Stator Slot Structure Effects on Efficiency, World Academy of Science, Engineering and Technology 77, 2011.

[15] **Admotec Inc.,** 1998. Understanding Resolvers and Resolver-to-Digital Conversion, Advanced Motion Technology, Technical Notes, January 1998.

CURRICULUM VITAE

Candidate's full name : Kadir ERDEM

Place and date of birth : İstanbul, 24.12.1984

Permanent Address : Fevzi Çakmak Mahallesi 1120 Sokak No:69 Daire:6
Esenler / İstanbul / Türkiye

Bachelor of Science : Yeditepe University, Istanbul, Turkey
Electrical and Electronic Engineering 2002-2008,
Double Major in Mechanical Engineering, 2004 - 2008